ORNL/TM-2022/1831

Assessment of Core Physics Characteristics of Extended Enrichment and Higher Burnup LWR Fuels using the Polaris/PARCS Two-Step Approach

Vol. I: PWR Fuel

Jianwei Hu
Ugur Mertyurek
William A. Wieselquist

June 2022

OAK RIDGE National Laboratory

ORNL IS MANAGED BY UT-BATTELLE LLC FOR THE US DEPARTMENT OF ENERGY

ORNL/TM-2022/1831

Nuclear Energy and Fuel Cycle Division

ASSESSMENT OF CORE PHYSICS CHARACTERISTICS OF EXTENDED ENRICHMENT AND HIGHER BURNUP LWR FUELS USING THE POLARIS/PARCS TWO-STEP APPROACH

VOL. 1: PWR FUEL

Jianwei Hu, Ugur Mertyurek, William A. Wieselquist

June 2022

Prepared by
OAK RIDGE NATIONAL LABORATORY
Oak Ridge, TN 37831-6283
managed by
UT-BATTELLE LLC
for the
US DEPARTMENT OF ENERGY
under contract DE-AC05-00OR22725

CONTENTS

FIGURES

TABLES

ABBREVIATIONS

ATF	accident-tolerant fuel
ARI	all (control) rods in
ARO	all (control) rods out
BOC	beginning of cycle
BWR	boiling water reactor
CRW	control rod worth
DTC	Doppler temperature coefficient
EE	extended enrichment
EFPD	effective full-power day
EOC	end of cycle
HALEU	high-assay low-enriched uranium
HFP	hot full power
HZP	hot zero power
IFBA	integral fuel burnable absorber
LEU	low-enriched uranium
LEU+	low-enriched uranium plus
LWR	light water reactor
MTC	moderator temperature coefficient
NRC	US Nuclear Regulatory Commission
ORNL	Oak Ridge National Laboratory
pcm	per cent mille
ppm	parts per million
PWR	pressurized water reactor
SDM	shutdown margin
SNC	Southern Nuclear Company
T/H	thermal-hydraulics
WABA	wet annular burnable absorber
WBN1	Watts Bar Nuclear Unit 1
WRSO	worst (control) rod stuck out
ZPPT	zero power physics tests

EXECUTIVE SUMMARY

Nuclear fuel with extended enrichment (^{235}U enrichment within 5–8 %), referred to as *low-enriched uranium (LEU) plus (LEU+)* in this report, is one of the evolutionary changes that has been pursued in recent years by commercial light water reactor operators and fuel vendors to improve the fuel cycle economy and operation performance of a nuclear plant. Higher fuel enrichments allow the fuel to be depleted to higher burnups than what is currently possible. This report assesses the impacts of LEU+ and higher burnup in pressurized water reactor (PWR) fuels on core physics characteristics using the Polaris/PARCS two-step approach. A representative LEU+ (with 5.95–6.6% enrichments) PWR core with a 24-month fuel cycle developed by Southern Nuclear Company was modeled with Polaris/PARCS using this two-step approach. To provide a comparison basis for the LEU+ core, a representative 18-month fuel cycle LEU (with 4.2–4.6% enrichments) PWR core was also modeled using a realistic core design. The total core power and total UO_2 loading were assumed to be the same for both cores in the PARCS models. As expected, significantly more burnable poison absorbers were used in the LEU+ core to accommodate its higher fuel enrichment. Nine different fuel assembly types were modeled via Polaris for each core to generate the lattice-average cross sections, which were then processed with GenPMAXS to prepare the nodal cross section data for PARCS. The PARCS results show that the average specific powers in all three fuel batches in the LEU+ core were similar to the corresponding fuel batches in the LEU core when the total core powers and total uranium loadings in both cores were the same. PARCS models were developed to simulate the steady-state operations of both cores. PARCS results for the LEU+ core were first compared with the corresponding VERA results in order to identify any significant modeling discrepancies. Although simplified core and fuel models were used in PARCS, good agreement between VERA and PARCS results were observed for soluble boron curve and core burnup distributions. Core physics parameters calculated with PARCS for zero power physics tests, beginning of cycle (BOC) conditions, and end of cycle conditions (EOC) were compared between the LEU+ core and the LEU core, including the soluble boron concentration, burnup distributions, assembly and pin power peaking factors, Doppler temperature reactivity coefficients, moderator temperature and density reactivity coefficients (MTC), control rod worth (CRW), and shutdown margin (SDM).

The main core physics characteristics of both cores are summarized in Table 11 (Section 5). Based on the core modeling results of this work, the main differences in PARCS results between the LEU+ and the LEU cores are summarized as follows.

- The critical boron concentrations were significantly higher in the LEU+ core than in the LEU core after ~100 effective full-power days in a cycle (e.g., 1582 vs. 1335 ppm for peak values).
- Higher assembly radial power peaking factors (1.40 vs. 1.30 for peak values), 2D pin peaking factors (1.53 vs. 1.42 for peak values), and 3D pin peaking factors (1.89 vs. 1.81 for peak values) were found in the LEU+ core compared to the LEU core.
- Significantly higher MTCs (-8.80 vs. -5.11 pcm/K at ZPPT) were found for the LEU+.
- Significantly lower CRW at EOC (e.g., 531 vs. 782 pcm for bank D) was found in LEU+ for all but one control bank.
- Lower SDMs (e.g., 5948 vs. 6503 pcm at EOC) were found in the LEU+ core.

This report also provides a demonstration of the current state of the Polaris/GenPMAXS/PARCS code suite in modeling PWR cores under steady-state operations. This work also contributed to Polaris/GenPMAX/PARCS improvements by providing feedback on code performances and also feature requests for a core physics study based realistic core designs.

Keywords: extended enrichment, higher burnup, LEU+, PARCS, core simulation, Polaris, GenPMAXS

1. INTRODUCTION

Nuclear fuel with extended enrichment (^{235}U enrichment within 5–8 wt%), referred to as *low-enriched uranium (LEU) plus (LEU+)* in this report, is one of the evolutionary changes that has been pursued in recent years by commercial light water reactor (LWR) operators and fuel vendors to improve the fuel cycle economy and operation performance of a nuclear plant. Higher fuel enrichments allow the fuel to be depleted to higher burnups than what is currently possible. Other fuel design changes are often required to accommodate the changes in enrichments, such as the higher loading of burnable poison absorbers. The effects of these changes on core physics parameters must be clearly understood to ensure the safe operation of these new fuel designs. The Polaris/PARCS [1] [2] [3] two-step approach is one of the approaches that is used by US Nuclear Regulatory Commission (NRC) to perform core modeling and simulations for regulatory reviews.

As part of the NRC-sponsored study on the impacts of LEU+ fuel on pressurized water reactor (PWR), boiling water reactor (BWR), and transition cores, this report assesses the impacts of LEU+ and higher burnup in PWR fuels on core physics characteristics using the Polaris/PARCS two-step approach. This work has built upon previous work at Oak Ridge National Laboratory (ORNL) that performed assembly-level assessments via Polaris for assembly designs with LEU+ and/or accident-tolerant fuel (ATF) materials for PWRs [4] and BWRs [5]. In this work, a representative PWR LEU+ core with a 24-month fuel cycle developed by Southern Nuclear Company (SNC) [6] was modeled using this two-step approach. To provide a comparison basis for the LEU+ core physics characteristics, a representative 18-month fuel cycle LEU PWR core design was also modeled using a realistic core design. Nine different fuel assembly types were modeled with Polaris for each core to generate the assembly cross sections, which were then processed with GenPMAXS [7] to prepare the nodal cross section data for PARCS. PARCS models were developed to simulate the steady-state operations of both cores. PARCS results for the LEU+ core were first compared with the corresponding VERA results (obtained from a separate project) in order to identify any significant modeling discrepancies. Core physics parameters calculated with PARCS for zero power physics tests (ZPPT[1]), beginning of cycle (BOC) conditions, and end of cycle (EOC) conditions were compared between the LEU+ core and the LEU core, including the soluble boron concentration, burnup distributions, assembly and pin power peaking factors, Doppler temperature reactivity coefficients (DTC), moderator temperature and density reactivity coefficients (MTC), control rod worth (CRW), and shutdown margins (SDMs).

As a module in SCALE [8], Polaris provides a 2D lattice physics analysis capability for LWR fuel designs. Polaris uses the method of characteristics (MOC) to solve the neutron transport, with resonance self-shielding treated using an embedded self-shielding method (ESSM). The ORIGEN depletion and decay code is integrated in Polaris to perform depletion calculations [8]. In this work, Polaris was used to simulate the depletion of the two sets of assembly types used in the LEU+ and LEU cores at various reactor operating conditions; branches were employed to generate cross sections for PARCS core simulations, and these cross sections are archived into "t16" files generated by Polaris. Polaris as available in SCALE version 6.3beta16 (with 56-group cross-section library based on ENDF/B-VII.1 data) was used in this work.

GenPMAXS is a code that processes the macroscopic cross section libraries and results of lattice physics codes—such as Polaris, HELIOS, TRITON, and CASMO—to generate PMAXS files, which provide PARCS with the nodal cross section data needed to perform core simulations for steady-state and transient conditions [7]. GenPMAXS version 6.3.1 was used in this work.

[1] Zero core power and zero Xe/Sm concentrations were used in ZPPT cases studied in this work, whereas equilibrium Xe/Sm concentrations were used in the BOC and EOC cases. See Section 4.5 for more details.

PARCS is a 3D reactor core simulator that solves the steady-state and time-dependent multigroup neutron diffusion or low-order neutron transport equations in Cartesian or hexagonal fuel geometries [3]. PARCS offers three options for thermal-hydraulics (T/H) fluid modeling: (1) simple single-phase treatment; (2) two-phase T/H model called PARCS Advanced Thermal Hydraulic Solver, and (3) coupling with an external T/H system analysis code, such as TRACE [9] or RELAP5 [10]. PARCS can perform the reactor kinetics calculations with T/H feedback [3]. PARCS version 3.3.6 with simple single-phase T/H treatment was used in this work. In particular, PARCS's capabilities relevant for this work include equilibrium cycle search, explicit Xe and Sm depletion, and critical boron search.

2. LEU+ AND LEU CORE DESIGNS AND MODELS

2.1 CORE LAYOUTS AND SHUFFLING SCHEMES

This work used a representative PWR LEU+ core designed by SNC [6]. The core had "flip-flop" equilibrium cycles, which are reached when a set of two consecutive core layouts repeat continuously. This set includes one core with an even number of fresh assemblies (referred to as "even cycle") and another core with an odd number of fresh assemblies (referred to as "odd cycle"), where the odd cycle includes a fresh assembly at the core center that remains there for both cycles. This core is designed to have a 24-month fuel cycle length. Figure 1 and Figure 2 show the shuffling scheme and the core layout, respectively, for the LEU+ core for the odd cycle. Figure 3 and Figure 4 show the shuffling scheme and the core layout, respectively, for the LEU+ core for the even cycle. All core layouts shown in this report are in quarter-core symmetry unless noted otherwise. Each cell in these four figures represents a fuel assembly. The meaning of the values and colors shown in each cell is provided in the legend. The LEU+ core uses a three-batch fuel shuffling scheme: fresh, once-burned, and twice-burned assemblies. For the burned assemblies, their locations in the previous cycle were modified from the SNC design to their corresponding locations in the current core quadrant (i.e., the south east quadrant) being modeled, given that quarter-core symmetry is used in this work. A typical low-leakage "ring-of-fire" layout (i.e., the ring is one assembly away from the core periphery) is used to arrange the fresh assemblies along the outer ring of the core, whereas the central part of the core is filled with fresh and once-burned assemblies arranged in a checkerboard pattern. The core periphery locations are filled with once- and twice-burned assemblies. The core layouts are similar between the odd and the even cycles with one distinct exception: the odd core cycle has a fresh assembly at the core center, whereas the even cycle does not.

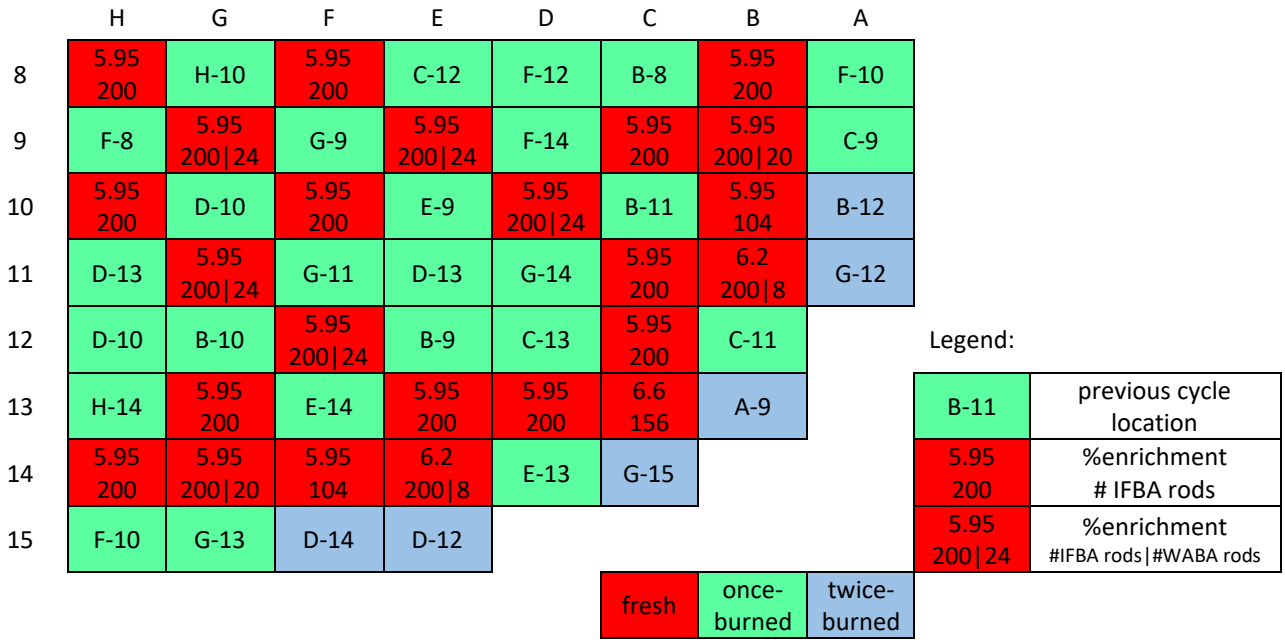

Figure 1. Fuel shuffling scheme of the LEU+ core (the odd cycle) in quarter-core symmetry.

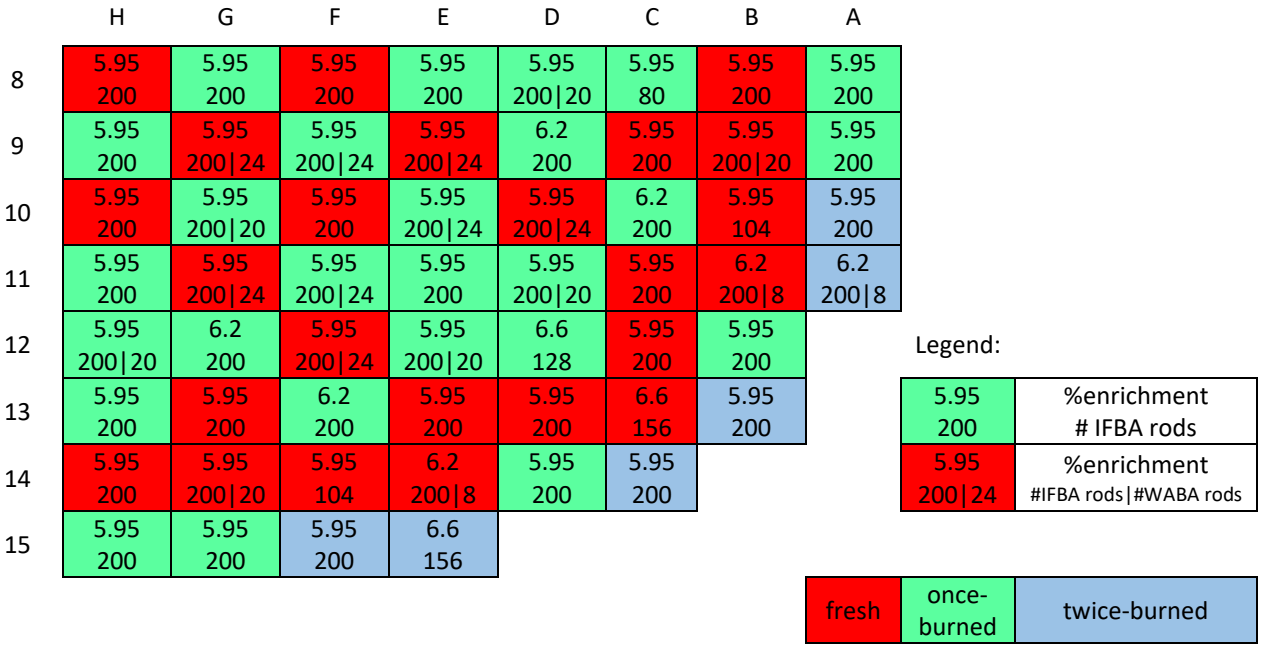

Figure 2. Core layout of the LEU+ core (the odd cycle) in quarter-core symmetry.

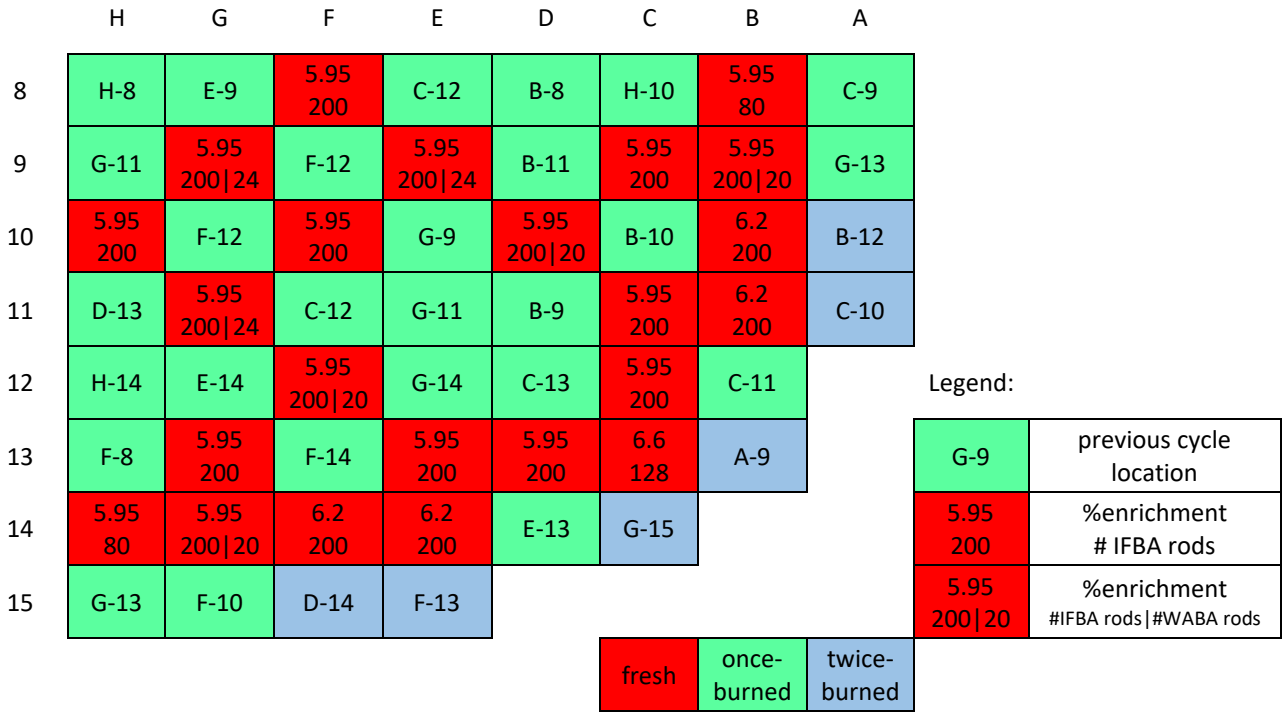

Figure 3. Fuel shuffling scheme of the LEU+ core (the even cycle) in quarter-core symmetry.

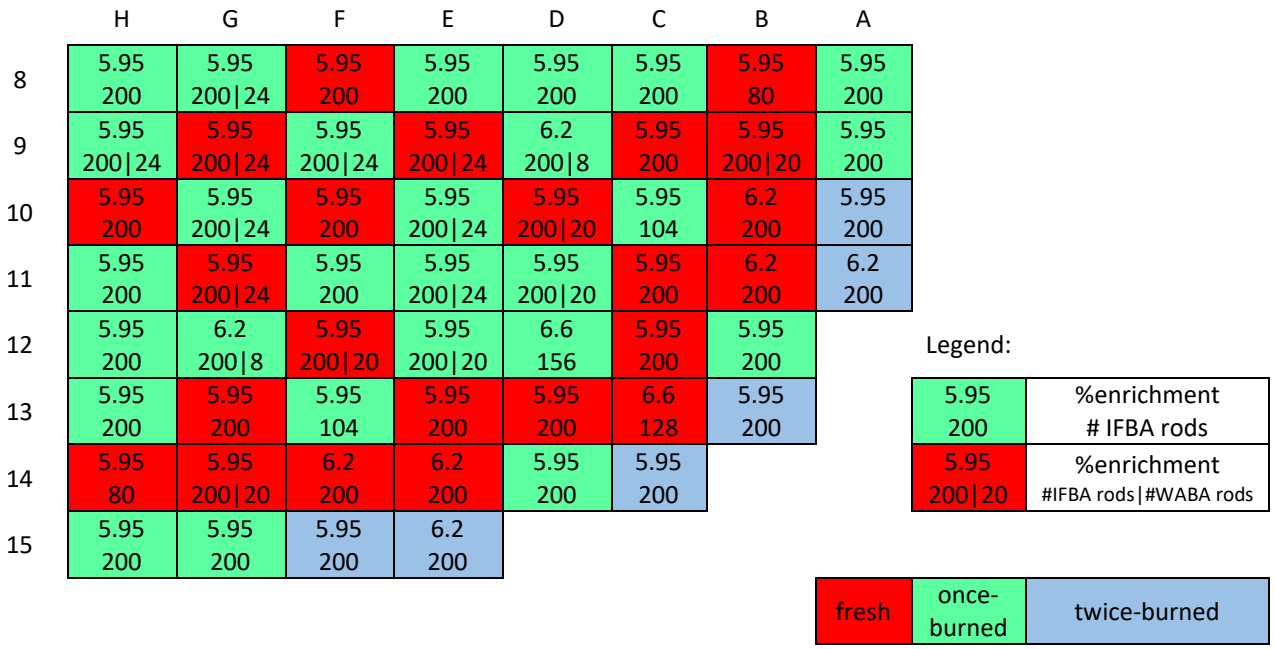

Figure 4. Core layout of the LEU+ core (the even cycle) in quarter-core symmetry.

As shown in Figure 1 to Figure 4, this LEU+ core design uses these three enrichments—5.95, 6.2, and 6.6% among different assemblies—which are significantly higher than what is used in current LWRs that is limited to less than 5%. This core uses these four different numbers of integral fuel burnable absorber (IFBA) rods—80, 104, 156, and 200—although most of the assemblies use 200 IFBAs. Three different

numbers of wet annular burnable absorber (WABA) rods—8, 20, and 24—are used in this core. WABA rods are only inserted in the fresh assemblies, although the numbers of WABA rods are also shown in the burned assemblies in the core layouts for which the WABA rods were only inserted when the hosting assemblies were fresh, and they were withdrawn in the current cycle. The effect of WABA rod insertions in the previous cycle was also accounted for this work. The detailed designs and specifications of these assemblies are discussed in Section 3.2.

Figure 5 and Figure 6 show the shuffling scheme and the core layout, respectively, for the LEU core, which was modified in this work from a realistic core design. The modifications include replacing several assemblies from a different reactor unit or from several cycles prior with assemblies from the previous cycle of this unit. Such modifications simplified the modeling process of this core while preserving the essence of the LEU core design. Although this LEU core is no longer in an equilibrium cycle (e.g., more once-burned assemblies than fresh assemblies) after the modifications, this core still represents a realistic core design and is assumed to be in an equilibrium cycle in this work to provide a comparison basis for the LEU+ core. This core is designed to have an 18-month fuel cycle, which is typical for current LWRs. This LEU core also uses a three-batch fuel shuffling scheme: fresh, once-burned, and twice-burned assemblies. This core is assumed to have just one equilibrium cycle (compared with the odd/even equilibrium cycles that the LEU+ core has). Similar to the LEU+ core, a typical ring-of-fire layout is used with fresh assemblies placed along the outer ring of the core, and a checkerboard pattern was used to fill the central part of core with fresh and once-burned assemblies. The core periphery positions are all filled with burned assemblies. All burned assemblies are assumed to be shuffled from the immediate previous cycle to simplify the models.

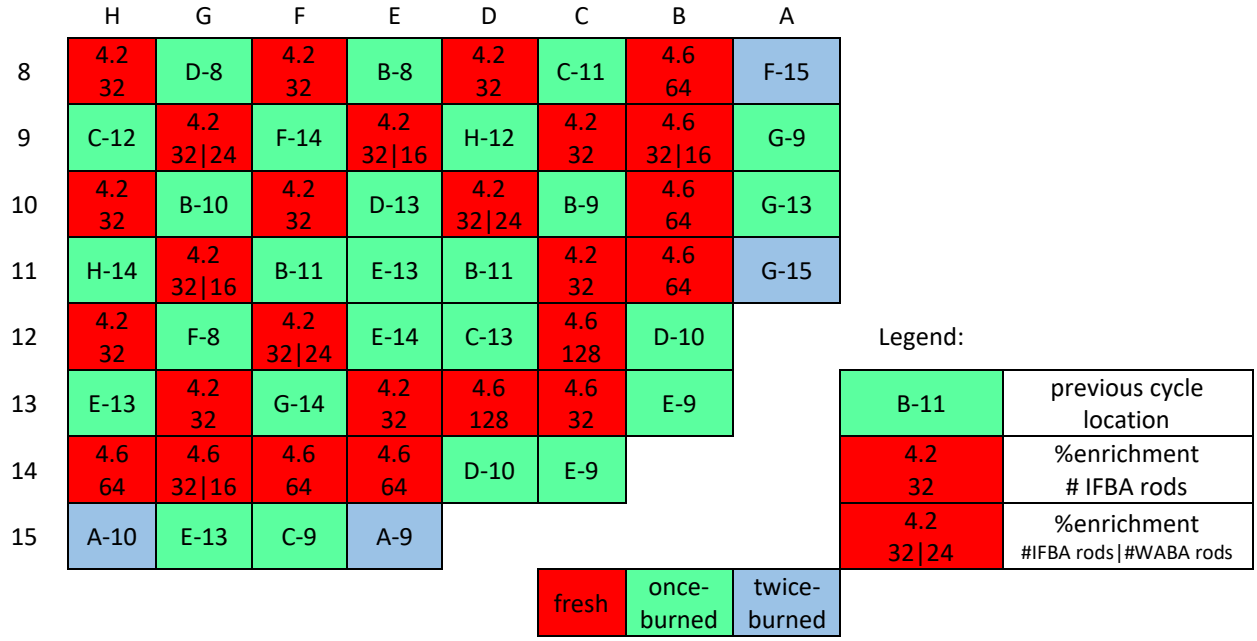

Figure 5. Fuel shuffling scheme of the LEU core in quarter-core symmetry.

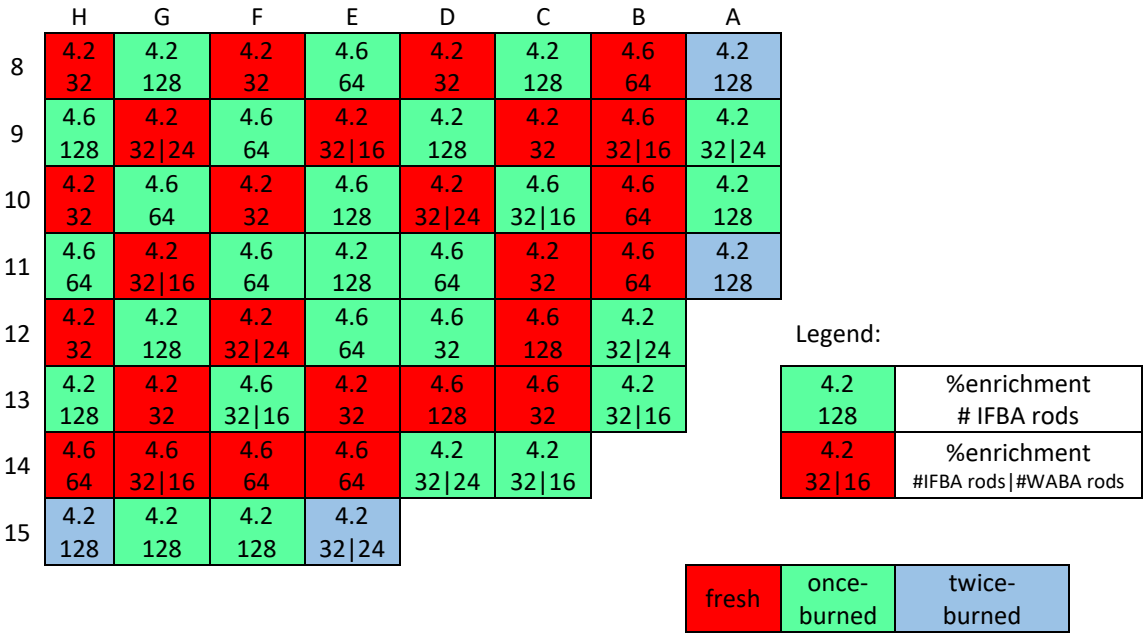

Figure 6. Core layout of the LEU core in quarter-core symmetry.

As shown in these two figures, this LEU core design uses two enrichments, 4.2 and 4.6% among different assemblies, which are significantly lower than what is used in the LEU+ core. This core uses three different numbers of IFBA rods—32, 64, and 128—although most of the assemblies use 32 IFBAs. Two different numbers of WABA rods—16 and 24—are used in this core. Similar to the LEU+ core, the WABA rods are inserted only in the fresh assemblies. Comparisons of the core layouts between LEU and LEU+ illustrated in Figure 1 to Figure 6 clearly show that significantly more IFBA and WABA rods are used in the LEU+ core than in the LEU core. This is expected because higher amounts of burnable absorber are needed to suppress the higher excess reactivity in the LEU+ core due to its higher fissile material loading. The detailed designs and specifications of the LEU assemblies are discussed in Section 3.2.

Table 1 summarizes the number of fuel assemblies in each of the three fuel batches for both the LEU and the LEU+ cores. Significantly fewer fresh assemblies are used in the LEU+ core than in the LEU core because of the use of higher enrichments in the LEU+ core even with the cycle length increased from 18 to 24-months. The LEU+ core also has less once-burned assemblies, and more twice-burned assemblies than the LEU core.

Table 1. Number of assemblies of each fuel batch for the LEU and LEU+ cores [6].

Batch type	LEU	LEU+ (odd cycle)	LEU+ (even cycle)
Fresh	89	85	84
Once-burned	92	84	85
Twice-burned	12	24	24
Total	193	193	193

Figure 7 shows the control bank layout [6], which is the same for both the LEU and LEU+ cores that were modeled in this work. Nine different control banks (identified as A, B, etc. in Figure 7) are used in this design. Comparing Figure 7 with Figure 2 shows that for the LEU+ core, the D-8 and H-12 locations

reserved for SE control bank in the southeast quadrant are filled with assemblies that had WABA inserted in their previous cycles, which has special implications for the PARCS modeling discussed in Section 3.1. Similarly, comparing Figure 7 with Figure 6 shows that for the LEU core, the B-12 and D-14 locations in the southeast quadrant reserved for SA control bank are filled with assemblies that had WABA inserted in their previous cycles.

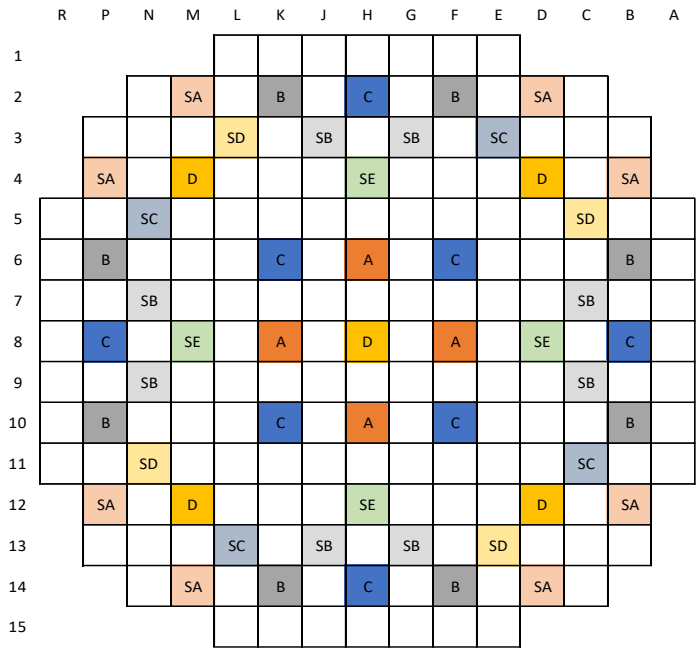

Figure 7. Control bank layout for the LEU and the LEU+ core modeled in this work [6].

Table 2 lists the main reactor parameters used in the PARCS models for both the LEU and LEU+ cores. The average assembly power was derived by dividing the core power of 3,626 MW by the total number of fuel assemblies (193) in the core. The fourth and fifth parameters shown in this table are from models used for the Watts Bar Nuclear Unit 1 (WBN1) [11]. The "MCYCLE" feature in PARCS was used to simulate the fuel shuffling and depletion of each cycle. Due to a limitation in the current version of code, PARCS cannot handle a full depletion cycle right after fuel shuffling in a single input, two separate PARCS inputs were used to simulate one fuel cycle in PARCS with one input for the shuffling and the other input for the depletion. The history file was used to pass information among inputs. Nine cycle iterations were used in both the LEU and the LEU+ cases to converge the burnup distributions—and hence power distributions—in the cores between two subsequent cycles, even though the burnup distributions were observed to have converged after smaller cycle iterations in some scenarios. A different convergence strategy was used for the LEU+ core because the core layouts between two subsequent cycles are different due to its use of the flip-flop cycles; thus, the burnup distributions between the two subsequent cycles are not expected to converge. However, by iterating the cycles nine times, the burnup distributions in an even cycle near the end of the iteration were observed to have converged with the previous even cycle. A similar observation was made for the odd cycles.

Table 2. Reactor parameters used in the PARCS model for the LEU and LEU+ cores [6] [11].

Parameters	Value
Total core thermal power	3626 MW
Average assembly power	18.7876 MW
U loading/assembly	0.465 MT
Inlet moderator temperature	564.82 K
Flow rate per assembly	85.963 kg/s
Gap conductance (W/m^2-s)	8,000 W/cm^2-s

Radial and axial reflector cross sections previously generated for WBN1 were used in the LEU and LEU+ cores in the PARCS models. The radial reflector comprised mostly water. The top reflector was 36.226 cm tall and included the plenum, spacer grid, and top nozzle, and so on. The bottom reflector was 16.951 cm tall and included the bottom nozzle, gap, etc. The active core was assumed to be 365.76 cm tall, and the spacer grids in the active core region were ignored for simplicity because the main purpose of this work was to assess the difference in PARCS results between the LEU and the LEU+ cores.

3. ASSEMBLY MODELS AND DESIGN SPECIFICATIONS

3.1 POLARIS ASSEMBLY MODELS

For the LEU+ core, as shown in Figure 2, assemblies with nine different combinations of enrichments, number of IFBA rods, and number of WABA rods are used to fill the core. Figure 8 shows eight of the nine assembly configurations (in quarter-assembly symmetry) for the LEU+ core, because one of the assembly configurations is shared by two different enrichments. All assemblies used in the LEU+ and LEU cores are assumed to have the standard Westinghouse 17 × 17 assembly design. As indicated in the captions, three of the five IFBA layouts were taken from Sanders and Wagner [12], and the remaining two layouts were designed in this work by using what is available in Sanders and Wagner [12] as a guide. For the assembly configurations with less than 156 IFBAs, most of IFBAs were placed adjacent to the guide tubes and the instrumentation tube to reduce the power peaking due to the extra moderation in those locations. The three WABA layouts were taken from Godfrey [11]. The enrichment in the regular fuel rods and the IFBA rods was assumed to be uniform across a given assembly.

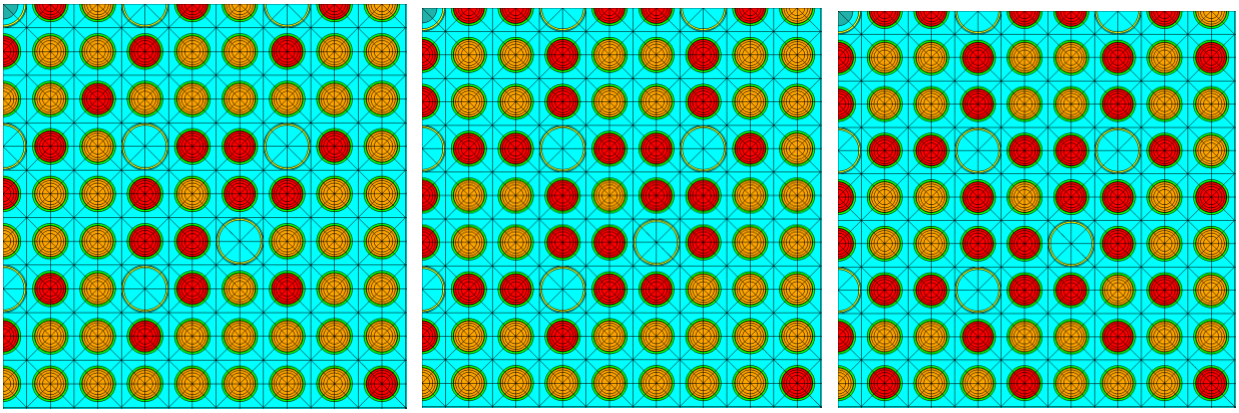

(a) 80 IFBAs (b) 104 IFBAs (c) 128 IFBAs

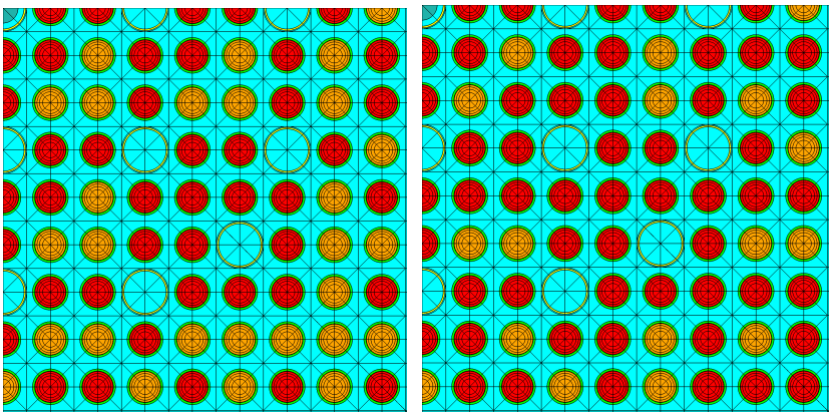

(d) 156 IFBAs (e) 200 IFBAs

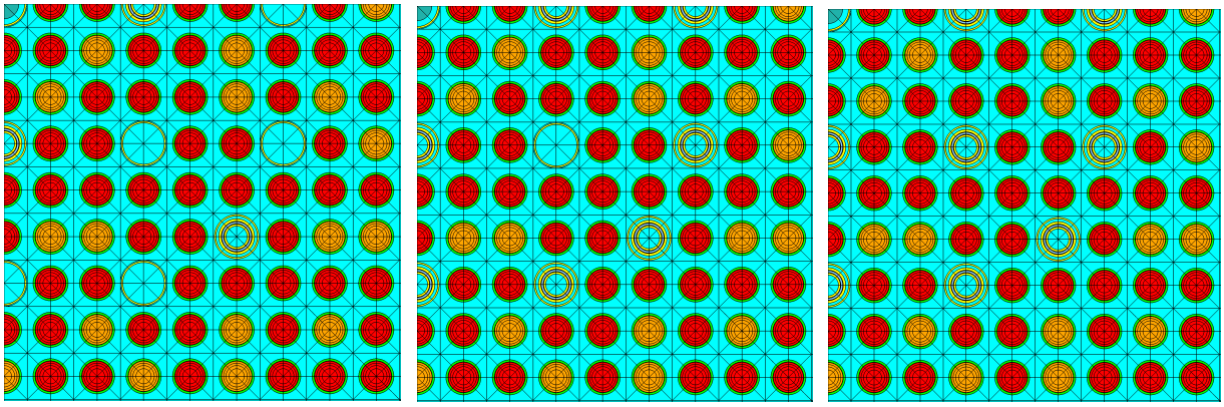

(f) 200 IFBAs with 8 WABA rods (g) 200 IFBAs with 20 WABA rods (h) 200 IFBAs with 24 WABA rods

Figure 8. Polaris models of the assembly configurations in quarter-assembly symmetry used in the LEU+ core (the IFBA rods are red): (a) 80 IFBAs [12], (b) 104 IFBAs [12], (c) 128 IFBAs, (d) 156 IFBAs [12], (e) 200 IFBAs, (f) 200 IFBAs with eight WABAs [11], (g) 200 IFBAs with 20 WABAs [11], and (h) 200 IFBAs with 24 WABAs [11].

For the LEU core, as shown in Figure 6, assemblies with nine different combinations of enrichments, number of IFBA rods, and number of WABA rods were used to fill the core. Figure 9 shows five of the nine assembly configurations for the LEU core, and several configurations are shared by different

enrichments. All three IFBA layouts shown in this figure were designed in this work by using what is available in Sanders and Wagner [12] as a guide. All WABA layouts were taken from Godfrey [11].

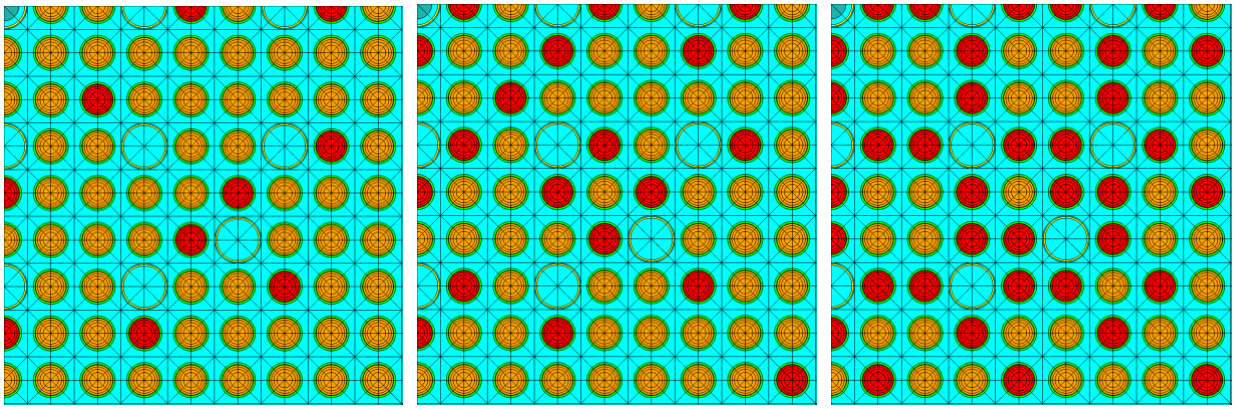

(a) 32 IFBAs (b) 64 IFBAs (c) 128 IFBAs

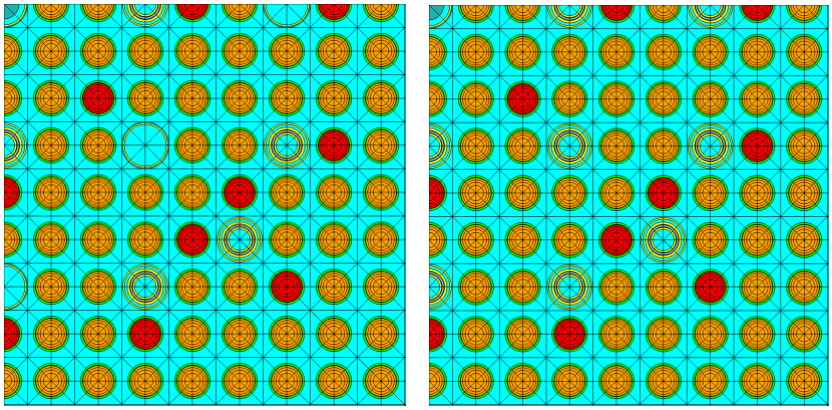

(d) 32 IFBAs with 16 WABA rods (e) 32 IFBAs with 24 WABA rods

Figure 9. Polaris models of the assembly configurations in quarter-assembly symmetry used in the LEU core (the IFBA rods are red): (a) 32 IFBAs, (b) 64 IFBAs, (c) 128 IFBAs, (d) 32 IFBAs with 16 WABAs [11], and (e) 32 IFBAs with 24 WABAs [11].

Depletion calculations were performed by using these assembly models with Polaris to a final burnup of 80 GWd/MTU to generate the cross sections required for the PARCS simulations. A 56-group cross-section library based on ENDF/B-VII.1 data was used in these Polaris calculations. For each of the nine assembly models, eight Polaris cases with different combinations of moderator temperature/density, soluble boron concentration, fuel temperature, and control rod insertion were simulated to generate cross sections that would cover the possible parameter space for PARCS to simulate reactor startup and normal operations. For each Polaris case without WABA rod insertions, 48 branches were used to accommodate different combinations of moderator temperature/density, soluble boron concentration, fuel temperature, and control rod insertion. For each Polaris case with WABA rod insertions, 63 branches were used to accommodate different combinations of moderator temperature/density, soluble boron concentration, fuel temperature, and control rod insertion. The 15 extra branches in the Polaris cases with WABA were used to simulate the scenario in which control rods were inserted instead of WABA, which are needed to simulate the several control assemblies, as discussed in Section 2.1, in both LEU and LEU+ cores that had WABA insertion in their previous cycle.

For the branch structure, four moderator (temperature, density) pairs were used: (293 K, 1.0052 g/cm^3), (550 K, 0.76971 g/cm^3), (585 K, 0.70045 g/cm^3), and (615 K, 0.60811 g/cm^3). Four fuel temperatures were used: 293, 560, 800, and 1,600 K. Four soluble boron concentrations were used: 0, 600, 1,800, and 2,500 ppm. Cross sections generated from these cases are interpolated by PARCS to generate the cross sections required for some particular combinations of these parameters to simulate the actual reactor conditions.

3.2 FUEL DESIGN PARAMETERS

Table 3 lists the design specifications for the IFBA rods and the regular fuel rods for both the LEU and LEU+ cores modeled in this work. These specifications were taken from Godfrey [11]. The IFBA rods have a 10 μm thick layer of ZrB_2 coated on the fuel pellet surface. The IFBA rod specifications were assumed to be the same as regular fuel rods in this work, except that the fuel-cladding gap in the IFBA rods was 10 μm smaller than that in the regular fuel rods. Some IFBA rod designs use annular blankets at the top and bottom of the rods, but those features were not modeled in this work for simplicity and the poison coating on IFBA rods was assumed to have the same height as the fuel stack. A 50 wt% ^{10}B enrichment of B was used in ZrB_2, and the total ^{10}B loading in IFBA rods was 2.353 mg/in. The density of UO_2 in all fuel rods was assumed to be 10.376 g/cm^3, which was based on 95.6% theoretical density [13] and a 1% factor to account for dishes and chamfers.

Table 3. Specifications of IFBA rods [11] and regular UO_2 rods used in both the LEU and LEU+ cores modeled in this work [11].

Item	Value
IFBA	
Poison (coating) material	ZrB_2
ZrB_2 density	3.85 g/cm^2
Coating inner radius	0.4096 cm
Coating thickness	10 μm
Coating density	3.85 g/cc
^{10}B enrichment	50 wt%
^{10}B loading	2.353 mg/in
Coating height	365.76 cm
Regular fuel rods	
Fuel material	UO_2
UO_2 density	10.376 g/cc
Fuel pellet radius	0.4096 cm
Cladding inner radius	0.418 cm
Cladding outer radius	0.475 cm
Rod pitch	1.26 cm
Assembly pitch	21.5 cm
Fuel stack height	365.76 cm

Table 4 lists the specifications of the control rods used in the control banks (Figure 7) for both the LEU and LEU+ cores, and Table 5 lists the specifications of the WABA rods. These specifications were taken from Godfrey [11], but the control rods were assumed to be filled with only B_4C for simplicity instead of a combination of B_4C and AIC used in WBN1. Boron-10 with 19.9% abundance (i.e., atom percentage) was used in the control rods, and ^{10}B with 19.7% abundance (i.e., atom percentage) was used in the WABA rods, which are also the default ^{10}B abundances used by Polaris for B_4C control rods and WABA rods, respectively.

Table 4. Specifications of the control rods used in both the LEU and LEU+ cores modeled in this work [11].

Item	Value
Poison material	B_4C
Poison density	1.76 g/cc
Cladding inner radius	0.386 cm
Cladding outer radius	0.484 cm
Poison height	360.68 cm
^{10}B abundance	19.9 atom%
Control rod withdraw step size	1.5875 cm
Axial location of poison (when fully inserted)	4.72 cm above the bottom of fuel stack

Table 5. Specifications of the WABA rods used in both the LEU and LEU+ cores modeled in this work [11].

Input	Value
Poison material	B_4C-Al_2O_3
^{10}B loading	6.03 mg/cm
Poison density	3.65 g/cc
Inner clad inner radius	0.286 cm
Inner clad outer radius	0.339 cm
Poison inner radius	0.353 cm
Poison outer radius	0.404 cm
Outer clad inner radius	0.418 cm
Outer clad outer radius	0.484 cm
Annulus material	Moderator
Cladding material	Zircaloy-4
Plenum/gap material	He

4. RESULTS

Once the cross-section files (t16 files) for each fuel assembly types were generated from the Polaris calculations, they were processed by GenPMAXS to generate the nodal cross section data for PARCS simulations. Before the cycle iterations described in Section 2.1 were performed by using PARCS to converge the burnup distributions in the core, two trial cycles were used to "jump start" the iteration, although there are other approaches to jump start the iteration. The first trial cycle used all fresh assemblies and depleted the core to a core average burnup of ~50 GWd/MTU, which provided assemblies with a range of burnups to mimic the once- and twice-burned assemblies. After shuffling the burned assemblies from the first cycle with desirable burnups to the appropriate core locations, the second trial cycle was used to deplete the core filled with fresh and burned assemblies to a core average burnup of ~28 GWd/MTU. The history file (*.parcs_cyc*) generated by the second trial cycle was fed into the first cycle of the nine-cycle iterations (Section 2.1), which in turn generated a history for the next cycle. This process was repeated until the iterations were completed. The history files contain all the information required to restart a PARCS core calculation, such as the burnup distributions, power peaking factors, the Xe/Sm distributions, and temperature distributions. It took ~40 min to complete the nine-cycle iterations with PARCS on one CPU on a Linux cluster.

This section presents the main core physics results from the PARCS calculations: the soluble boron concentrations, burnup distributions, power peaking factors, reactivity coefficient, CRW, and SDM. For brevity, only the results from the odd cycle are presented in this section for the LEU+ core because the even cycle results are similar, which are included in Appendix A. In addition to the comparisons of PARCS results between the LEU and LEU+ cores, the PARCS results on the LEU+ core are compared with the available VERA results to in order to identify any significant modeling discrepancies. PARCS and VERA used similar core maps and fuel shuffle patterns for the two odd- and even-cycle LEU+ cores modeled in this work; however, the PARCS and VERA core models differ in the following aspects: (1) the two LEU+ cores modelled in PARCS are true equilibrium cores, whereas the VERA models simulated a set of varying LEU+ cores (including the two subject LEU+ cores) after a series of transition-core cycles; (2) some fuel assembly design parameters (e.g., fuel density, pellet radius, IFBA layouts) used in the VERA models are proprietary and unavailable for this work; representative values are used for these parameters in the PARCS models; (3) the spacer grids in the active core region in the PARCS models were ignored, (4) the full core is modelled in the VERA models and only a quarter core is modelled in the PARCS models using quarter-core symmetry, (5) reflector cross sections were treated differently between the two sets of models, and (6) the short annular blankets, which have a hole in the middle and do not contain poisons, on both ends of IFBA rods included in the VERA models were not included in the PARCS models. The difference in the modeling of IFBA blankets resulted in ~1.5% higher total U loading and higher IFBA poison loading in the PARCS models than in the VERA models, even though the total number of IFBA rods is the same in both sets of models.

4.1 SOLUBLE BORON CURVE

The critical boron concentration in the moderator is an important indicator of the total core excess reactivity, which depends on several factors, including the core layout, the total amount and distribution of the fissile content (i.e., enrichment) in the assemblies, and the total amount and distribution of the burnable poisons in the assemblies. Figure 10 shows three sets of results for the critical boron concentrations: VERA results for the LEU+ core [6], PARCS results for the LEU+ core, and PARCS results for the LEU core. Good agreements are seen between the VERA and PARCS results for the LEU+ core, which indicates consistent core modeling has been used in both the VERA and PARCS calculations. Small differences in boron concentrations between VERA and PARCS are seen at the BOC and near EOC, which can be mainly attributed to the modeling differences mentioned above and methods used

between the PARCS and VERA calculations. For example, the higher amount of U loading and IFBA poison loading in the PARCS model than in the VERA model had a competing effect on the soluble boron concentrations. As U loading increases, critical boron concentration increases; on the other hand, as IFBA loading increases, critical boron concentration decreases. Longer cycle length (704 EFPDs) is seen in the PARCS results for the LEU+ core than that in the VERA results (693 EFPDs), which can be attributed to the higher U loading in the PARCS model. In all cases, the boron concentrations initially increased with EFPD, which was mainly due to burnout of the burnable poisons, such as IFBA and WABA. Much higher boron concentrations are seen in the LEU+ than in the LEU core, which is expected because higher boron concentrations are needed to suppress the higher excess reactivity provided by the higher average enrichment in LEU+. For example, the peak concentrations are 1,582 and 1,335 ppm for LEU+ and LEU, respectively, according to the PARCS results. The concentrations peak occurred much later (155 vs. 75 EFPD) in LEU+ than in LEU because of the higher burnable poison loading in LEU+. The concentrations declined at higher EFPDs because of the depletion of fissile content. The cycle length of the LEU core is estimated to be 514 EFPDs, which is right before k_{eff} decreases below 1.0 and the boron concentration decreases to zero (Figure 10).

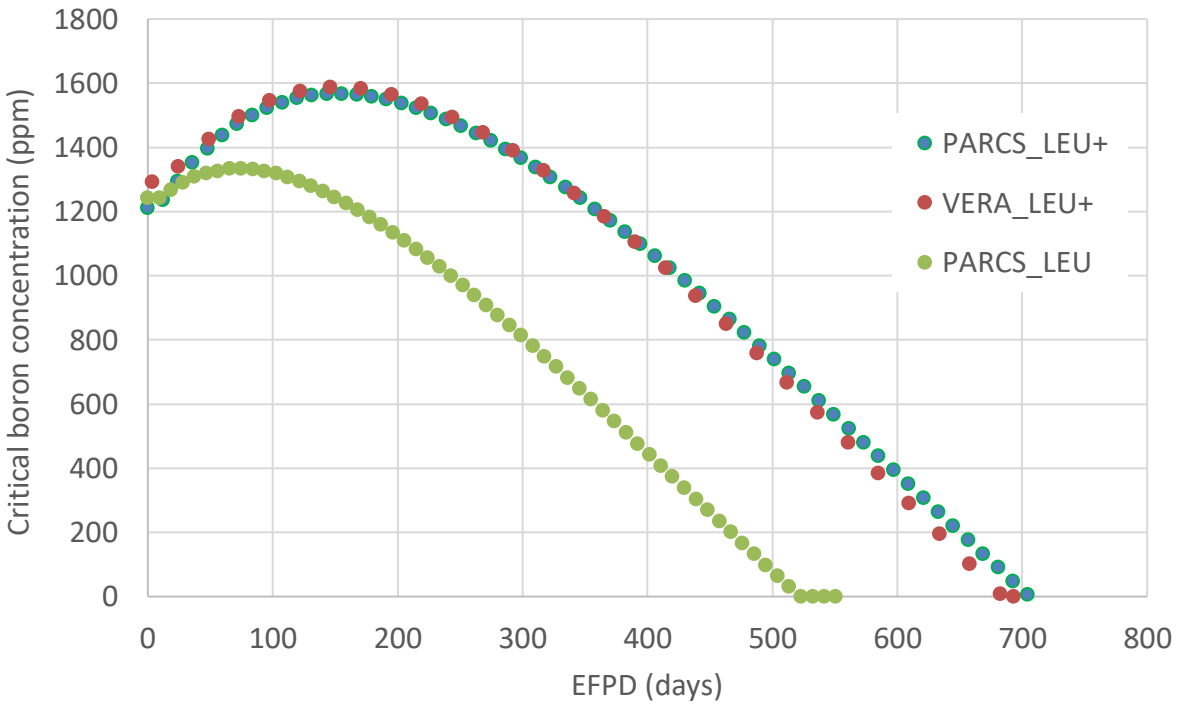

Figure 10. Critical soluble boron concentrations of the LEU and LEU+ cores calculated by PARCS and VERA.

4.2 BURNUP DISTRIBUTIONS

Figure 11 and Figure 12 compare the burnup distributions in the LEU+ core between the PARCS results and the VERA results at BOC and EOC, respectively. Note the coloring scale for burnup in each figure is specific to the figure in order to highlight the maximum burnup locations. Similar patterns and burnup values at the corresponding locations are seen between PARCS and VERA results.

	H	G	F	E	D	C	B	A
8	0.00	37.33	0.00	35.10	35.27	35.07	0.00	37.14
9	37.35	0.00	34.38	0.00	32.63	0.00	0.00	37.95
10	0.00	35.36	0.00	34.60	0.00	29.65	0.00	55.86
11	35.09	0.00	34.51	35.09	32.11	0.00	0.00	61.53
12	35.36	32.62	0.00	32.08	29.54	0.00	37.43	
13	35.10	0.00	29.65	0.00	0.00	0.00	53.11	
14	0.00	0.00	0.00	0.00	37.41	52.41		
15	37.14	37.91	55.89	62.22				

(a) PARCS

H	G	F	E	D	C	B	A
0	38.08	0	36.62	35.23	35.46	0	37.80
38.13	0	34.80	0	33.48	0	0	38.80
0	35.73	0	34.92	0	30.27	0	55.90
34.72	0	34.78	35.67	32.66	0	0	61.90
36.13	33.54	0	32.74	30.10	0	38.10	
35.48	0	30.24	0	0	0	52.60	
0	0	0	0	38.12	53.49		
37.31	38.77	55.88	62.42				

(b) VERA

Figure 11. The average burnup value (GWd/MTU) in each assembly at BOC in the LEU+ core (odd cycle) calculated by (a) PARCS and (b) VERA.

	H	G	F	E	D	C	B	A
8	37.38	68.24	37.55	65.08	64.57	65.66	33.49	52.87
9	68.21	35.18	66.07	34.27	63.92	37.95	32.07	53.05
10	37.39	66.71	37.10	64.92	34.81	63.17	33.53	67.88
11	64.98	34.17	64.82	63.76	63.05	37.59	29.07	70.46
12	64.61	63.89	34.81	63.02	62.50	34.81	55.53	
13	65.67	37.96	63.19	37.62	34.84	28.92	63.15	
14	33.49	32.09	33.59	29.17	55.57	62.52		
15	52.88	53.04	67.96	71.45				

(a) PARCS

H	G	F	E	D	C	B	A
38.20	68.44	38.29	66.02	64.10	65.57	34.30	53.20
68.47	35.68	66.10	34.66	64.36	38.74	32.71	53.50
38.25	66.75	37.67	64.70	35.05	63.60	34.10	67.60
64.49	34.67	64.60	63.64	62.96	38.10	29.49	70.40
64.84	64.39	35.06	63.05	62.48	35.29	55.70	
65.59	38.74	63.60	38.13	35.30	29.49	62.30	
34.31	32.75	34.18	29.60	55.70	63.18		
52.73	53.49	67.64	71.27				

(b) VERA

Figure 12. The average burnup value (GWd/MTU) in each assembly at EOC in the LEU+ core (odd cycle) calculated by (a) PARCS and (b) VERA.

Figure 13 compares the burnups accumulated during an odd equilibrium cycle in each assembly between PARCS and VERA, and the burnup accumulation ratio of PARCS to VERA ranges from 0.98 to 1.05, which can be considered good agreement, considering the differences between the PARCS and VERA models and methods. The distributions of burnup accumulations (EOC-BOC) shown in Figure 13 correlate well with the core layout shown in Figure 2; for example, the highest burnups are accumulated in the fresh assemblies, and the lowest burnups are accumulated in the twice-burned assemblies.

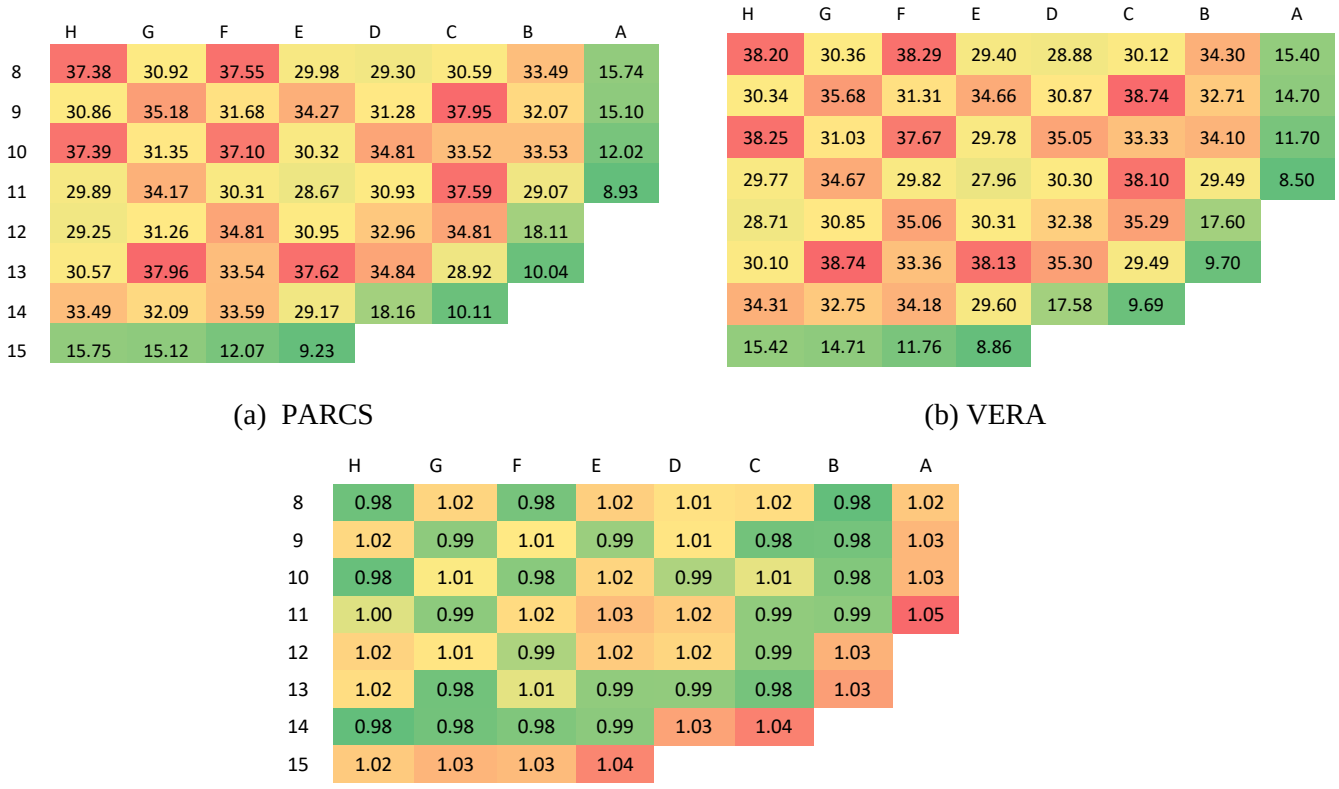

(a) PARCS

(b) VERA

(c) Burnup ratio of PARCS to VERA

Figure 13. The burnup (GWd/MTU) accumulated in an equilibrium cycle in each assembly in the LEU+ core (odd cycle) calculated by (a) PARCS and (b) VERA; (c) the ratio of burnup calculated by PARCS to that by VERA.

Figure 14 and Figure 15 compare the burnup distributions calculated by PARCS between the LEU+ and the LEU core at BOC and EOC, respectively. The burnup distributions at BOC are consistent with the corresponding three-batch core layouts for both the LEU+ (Figure 2) and the LEU (Figure 6) cores, showing higher burnups in twice-burned assemblies, lower burnups in once-burned, and zero burnups in the fresh assemblies. As expected, the burnup values in the LEU+ core are generally higher than in the corresponding burned assemblies in the LEU core at both BOC and EOC. For instance, at EOC the burnup values in the LEU+ core range from 28.92 to 71.45 GWd/MTU among different assemblies, whereas burnup values in the LEU core range from 22.72 to 51.63 GWd/MTU.

	H	G	F	E	D	C	B	A
8	0.00	37.33	0.00	35.10	35.27	35.07	0.00	37.14
9	37.35	0.00	34.38	0.00	32.63	0.00	0.00	37.95
10	0.00	35.36	0.00	34.60	0.00	29.65	0.00	55.86
11	35.09	0.00	34.51	35.09	32.11	0.00	0.00	61.53
12	35.36	32.62	0.00	32.08	29.54	0.00	37.43	
13	35.10	0.00	29.65	0.00	0.00	0.00	53.11	
14	0.00	0.00	0.00	0.00	37.41	52.41		
15	37.14	37.91	55.89	62.22				

(a) LEU+ (PARCS)

H	G	F	E	D	C	B	A
0.00	27.81	0.00	26.79	0.00	27.72	0.00	39.68
26.77	0.00	26.46	0.00	27.88	0.00	0.00	26.72
0.00	26.48	0.00	26.78	0.00	26.20	0.00	28.40
26.67	0.00	23.80	27.76	23.80	0.00	0.00	39.53
0.00	28.05	0.00	23.84	22.72	0.00	25.97	
27.76	0.00	26.09	0.00	0.00	0.00	27.26	
0.00	0.00	0.00	0.00	25.97	27.26		
39.72	27.76	28.40	38.85				

(b) LEU (PARCS)

Figure 14. The average burnup in each assembly at BOC calculated by PARCS in (a) the LEU+ core (odd cycle) and (b) the LEU core.

	H	G	F	E	D	C	B	A
8	37.38	68.24	37.55	65.08	64.57	65.66	33.49	52.87
9	68.21	35.18	66.07	34.27	63.92	37.95	32.07	53.05
10	37.39	66.71	37.10	64.92	34.81	63.17	33.53	67.88
11	64.98	34.17	64.82	63.76	63.05	37.59	29.07	70.46
12	64.61	63.89	34.81	63.02	62.50	34.81	55.53	
13	65.67	37.96	63.19	37.62	34.84	28.92	63.15	
14	33.49	32.09	33.59	29.17	55.57	62.52		
15	52.88	53.04	67.96	71.45				

(a) LEU+ (PARCS)

H	G	F	E	D	C	B	A
25.86	49.75	26.20	49.92	25.96	50.02	24.99	49.56
49.86	24.91	49.55	25.45	49.72	26.50	24.40	37.96
26.48	49.73	25.81	48.67	24.18	49.49	24.70	38.89
49.97	25.69	46.31	47.61	45.88	25.85	22.16	46.74
26.04	49.97	24.36	45.98	45.27	24.92	39.55	
50.05	26.51	49.44	25.89	24.94	21.15	35.91	
24.88	24.30	24.69	22.21	39.57	35.91		
49.47	38.66	38.84	46.20				

(b) LEU (PARCS)

Figure 15. The average burnup in each assembly at EOC calculated by PARCS in (a) the LEU+ core (odd cycle) and (b) the LEU core.

Figure 16 compares the PARCS results on the burnups accumulated during the cycle in each assembly between LEU+ and LEU. As expected, the distributions of burnup accumulations are consistent with the corresponding core layouts for both LEU+ (Figure 2) and LEU (Figure 6) with the highest burnups accumulated in the fresh assemblies and the lowest burnups accumulated in the twice-burned assemblies. The burnup accumulations in an equilibrium cycle in the LEU+ core range from 8.93 to 37.96 GWd/MTU, whereas the burnup accumulations in the LEU core range from 7.81 to 28.40 GWd/MTU. The average burnup accumulation was 28.43 GWd/MTU for the LEU+ core and 20.7 GWd/MTU for the LEU core.

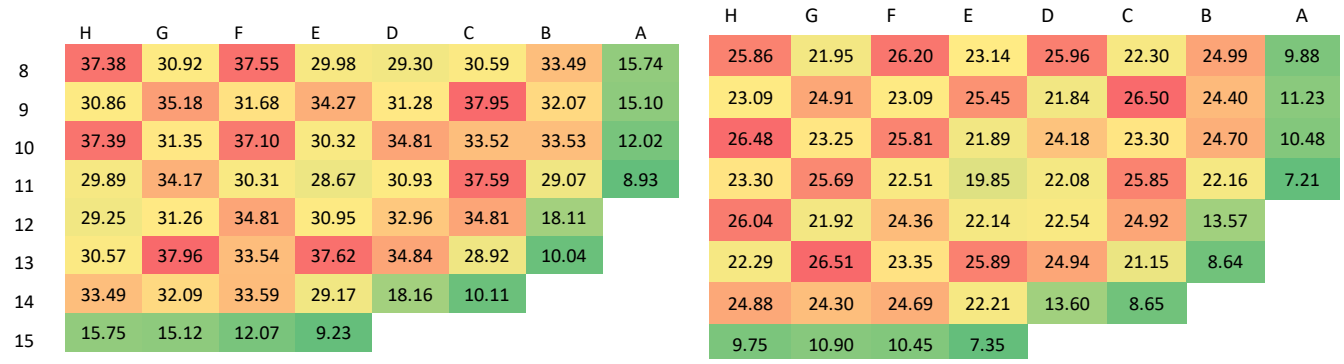

(a) LEU+ (PARCS) (b) LEU (PARCS)

Figure 16. The burnup accumulated in a cycle calculated by PARCS in each assembly in (a) the LEU+ core (odd cycle) and (b) the LEU core.

4.3 SPECIFIC POWER

One particular concern is how the use of higher enrichments affects the specific power experienced by each fuel batch in the LEU+ core compared with that in an LEU core. To address that concern, the PARCS burnup distribution results shown in Figure 16 are further analyzed here. After accounting for the quarter-core symmetry, the average burnup among the assemblies in each fuel batch and the core average burnup were calculated based on the burnup results shown in Figure 16. The average specific power among the assemblies of each fuel batch was derived by dividing the corresponding burnup by the effective full-power day (EFPD) of the cycle. In this derivation, the LEU+ core was assumed to have a 24- month fuel cycle with 704 EFPDs, and the LEU core was assumed to have an 18- month fuel cycle with 514 EFPDs. Both cores were assumed to have the same overall power (3626 MW) and the same total UO_2 loading. Table 6 summarizes the PARCS results for the cycle burnups and the specific power in each fuel batch in the LEU and LEU+ cores modeled in this work.

As shown in Table 6, higher burnup accumulations in a cycle are seen in the corresponding fuel batches in the LEU+ core than those in the LEU core, which are expected given the higher cycle length of the LEU+ core. The average specific power in the fresh assemblies in the LEU+ core is ~1% higher than those in the LEU core, which can be attributed to similar "ring of fire" layouts for fresh assemblies in both cores. The average specific power in the LEU+ core is ~10% higher for the once-burned assemblies and ~9% lower in the twice-burned assemblies than the corresponding assemblies in the LEU core, which can be attributed to the differences in core layouts between the two cores for the burned assemblies and thus different power distributions. The fuel (i.e., UO_2) density and total fuel volume are assumed to be the same in both cores, and thus the total UO_2 loading is the same in the two cores. However, the average ^{235}U enrichment is higher in the LEU+ core than the LEU core (6.0% vs. 4.4%), which leads to slightly lower total U loading in the LEU+ because ^{235}U atoms are slightly lighter than ^{238}U atoms. The combined effects of same overall core power and slightly lower U loading in the LEU+ core has led to the slightly higher (40.4 vs. 40.3) core-average specific power in the LEU+ core.

Table 6. PARCS results for burnup accumulated during a cycle and the cycle-average specific power in an assembly of each fuel batch in the LEU and an LEU+ cores modeled in this work.

	LEU		LEU+	
Fuel batch	**Burnup/cycle** GWd/MTU	**Specific power*** MW/MTU	**Burnup/cycle** GWd/MTU	**Specific power** MW/MTU
Fresh	24.8	48.3	34.3	48.8
Once-burned	18.4	35.8	27.6	39.2
Twice-burned	8.1	15.8	10.4	14.8
Core average	20.7	40.3	28.4	40.4

*Both cores are assumed to have the same overall core power and same total UO_2 mass in the PARCS models.

4.4 ASSEMBLY AND PIN POWER PEAKING FACTORS

Figure 17 shows the assembly radial power peaking factors for both the LEU+ and LEU cores as functions of EFPD. Assembly radial power peaking is the maximum assembly total power normalized by the average assembly power in the core. The power peaking can come from different assemblies at different time steps, because the power distributions in the core change during the cycle mainly due to different depletion rates of the fissile materials and burnable absorbers among different assemblies. For the LEU+ core, the PARCS results fluctuated in a range (between 1.30 and 1.40) similar to the VERA results for assembly radial power peaking, although they diverged after 155 EFPD, which can be attributed to their differences in fuel assembly and core models described at the beginning of Section 4. Higher assembly radial peaking factors are seen in LEU+ than in LEU, and PARCS predicted the maximum and average values to be 1.395 and 1.354, respectively, for the LEU+ core (in comparison of 1.304 and 1.285, respectively, for the LEU core).

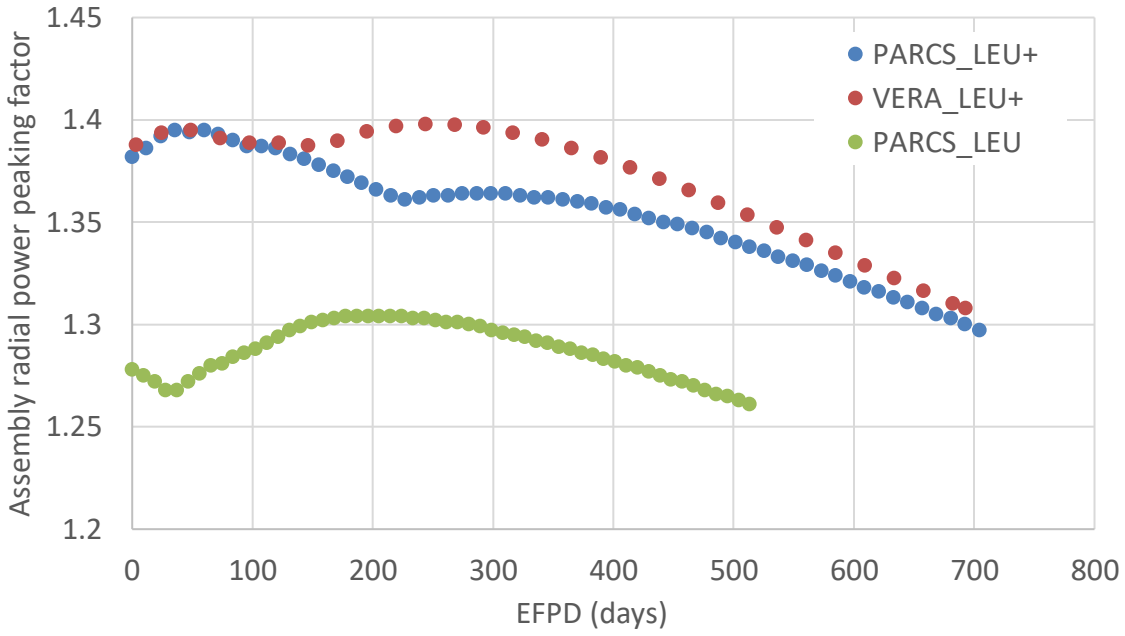

Figure 17. Assembly radial power peaking factor as a function of EFPD for the LEU and LEU+ cores calculated by PARCS and VERA.

Figure 18 and Figure 19 show the 2D and 3D pin power peaking factors as functions of EFPD for the LEU and LEU+ cores, respectively. A Python script was used to extract these factors from the PARCS output file (*parcs_cyc* file) because these two factors are not readily available from the PARCS output. The 2D peaking factor is the maximum of the radial pin peaking factor (based on total pin power) among all assemblies in the core. The 3D peaking factor is the maximum pin power in an axial pin segment normalized by the average power among all pin segments in the core. Higher magnitudes are seen in the 3D peaking factors (Figure 19) than in the 2D peaking factors (Figure 18), which is expected because the axial power shape introduces additional variations to the 3D factors. Similar to the radial assembly peaking factors, higher 2D and 3D pin peaking factors are seen in LEU+ than in LEU. The differences in these 2D and 3D peaking factor results between VERA and PARCS for the LEU+ core can be attributed to their differences in fuel assembly and core models described at the beginning of Section 4.

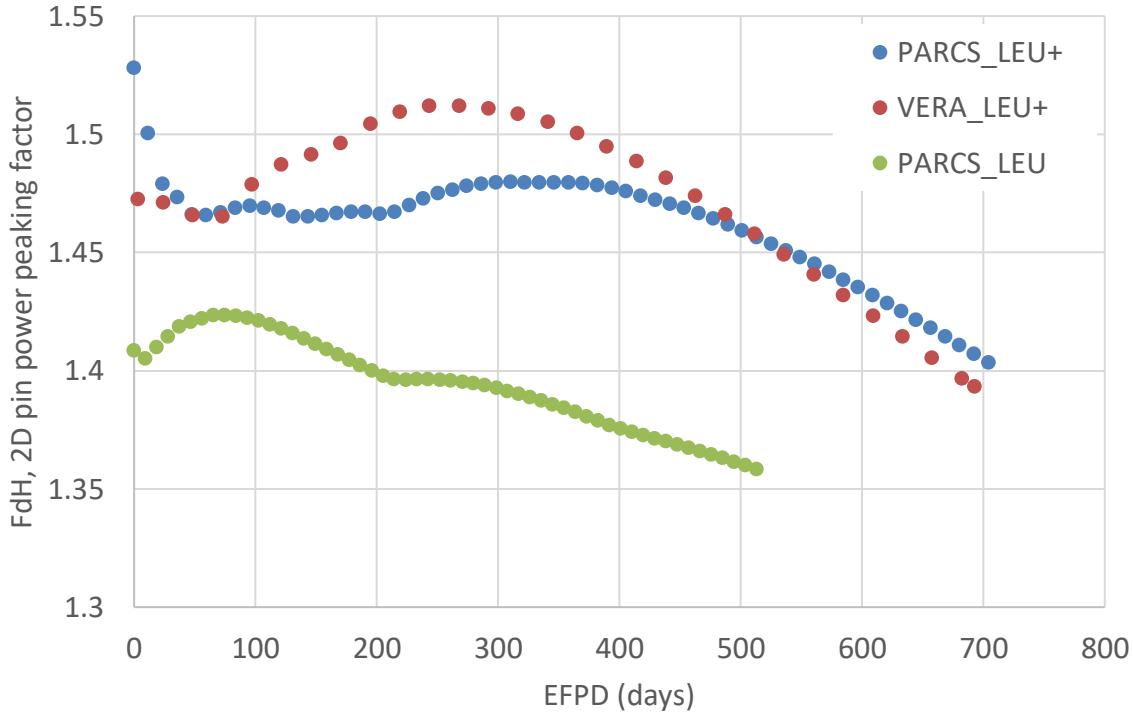

Figure 18. Maximum 2D pin power peaking factor (FdH) as a function of EFPD for the LEU and LEU+ cores calculated by PARCS and VERA.

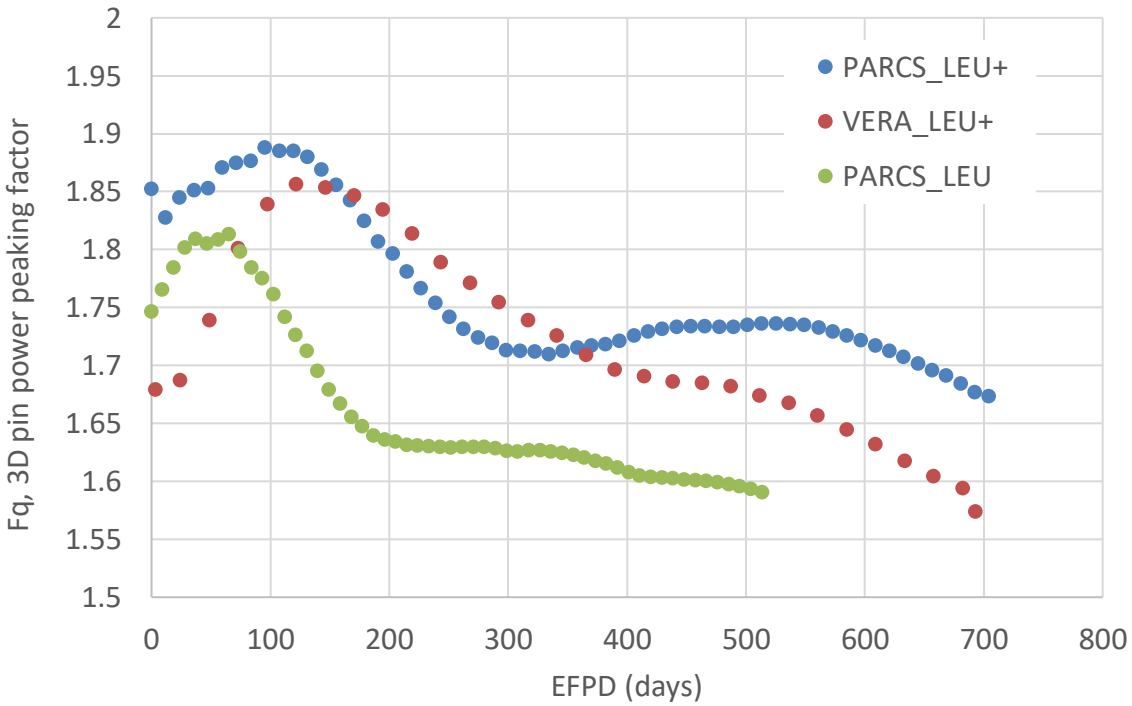

Figure 19. Maximum 3D pin power peaking factor (Fq) as a function of EFPD for the LEU and LEU+ cores calculated by PARCS and VERA.

4.5 REACTIVITY COEFFICIENTS, CONTROL ROD WORTH, AND SHUTDOWN MARGIN

The results in this section were all from the PARCS calculations for the LEU+ and the LEU core described in previous sections.

4.5.1 Fuel Temperature Reactivity Coefficients

Fuel temperature reactivity coefficients are often referred to as DTC because changes in fuel temperature affects Doppler broadening and thus reaction rates among different isotopes. Figure 20 and Figure 21 show reactivity, δk_{eff}, as a function of fuel temperature for the LEU+ core at ZPPT and EOC conditions, respectively. Reactivity (in pcm) is calculated using the following equation:

$$\delta k_{eff} = \frac{k_{eff}-1}{k_{eff}} \times 10^5 \quad \text{(Eq. 1)},$$

where k_{eff} is the core eigenvalue calculated by PARCS for a given case.

The trends of reactivity as a function of fuel temperature for the LEU core were nearly identical to the corresponding LEU+ results shown in Figure 20 and Figure 21 and thus are not plotted here. Zero core power and constant moderator temperature (565 K) and density were used in these all these ZPPT and EOC cases. For the ZPPT cases, the critical boron concentrations were calculated based on hot zero power (HZP) conditions. For the EOC cases, critical boron concentrations were calculated based on hot full power (HFP) conditions. Zero Xe and Sm concentrations were used in the ZPPT cases, whereas equilibrium Xe and Sm concentrations from the corresponding HFP conditions were used in the EOC cases. Table 7 summarizes the k_{eff} results at ZPPT and EOC for the LEU+ and the LEU cores. The table also includes the critical boron concentrations and DTCs. Core k_{eff} decreased in all four cases as fuel temperature increased from 560 to 590 K, which was expected because of the increased neutron absorption in the fuel as a result of Doppler broadening at higher fuel temperature. DTCs were determined by linearly fitting reactivity as a function of fuel temperature in Figure 20 and Figure 21. The equations and R^2 (indicating how well the data fits the trend line) of the fitting are also shown in the figures. As shown in Table 7, the k_{eff} are nearly identical between LEU+ and LEU at ZPPT, and thus the DTCs are close. The DTCs at EOC are slightly higher (i.e., more negative) in the LEU+ core than those in the LEU core. The DTCs at ZPPT were also found to be similar to the values reported in Godfrey [11]. Note that the k_{eff} values in Table 7 were significantly above 1.0 at EOC; this is because the moderator and fuel temperature used in these cases were significantly lower than those of the corresponding HFP core that yielded the critical boron concentration used in these cases. These results show an opposite trend for DTC with enrichment than the Phase 1 study [4], which shows lower magnitudes in DTC at higher enrichments. The differences can be attributed to the simplifications used in Phase 1 study, including (1) same burnable poison loading was used in different enrichment cases; (2) the soluble boron concentrations were assumed to be 0 in all cases.

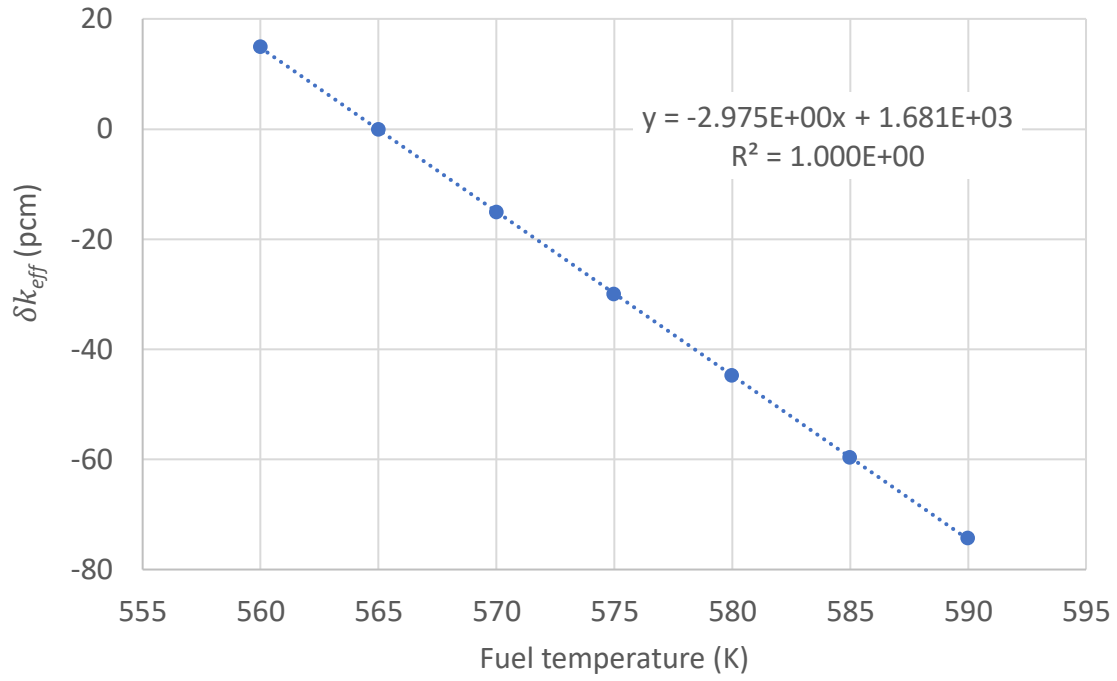

Figure 20. Reactivity as a function of fuel temperature calculated by PARCS for the LEU+ core at ZPPT.

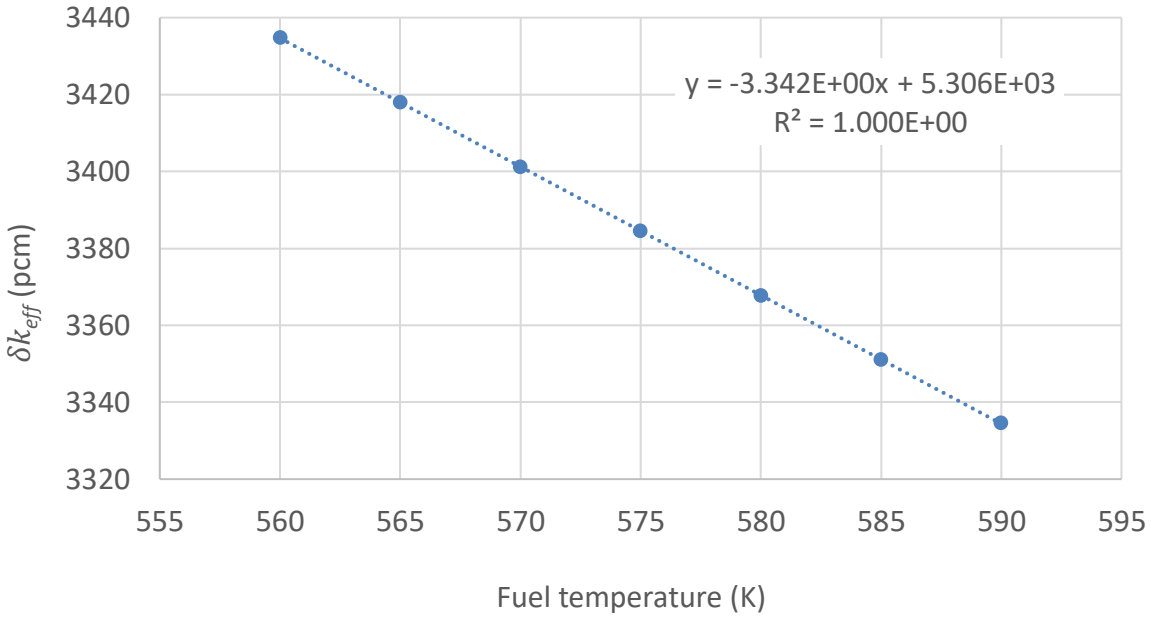

Figure 21. Reactivity as a function of fuel temperature calculated by PARCS for the LEU+ core at EOC.

Table 7. k_{eff} as a function of fuel temperature calculated by PARCS for the LEU and LEU+ cores at the ZPPT and EOC conditions. The critical boron concentrations and DTCs are also shown.

ZPPT			EOC		
	LEU	LEU+		LEU	LEU+
Tf (K)	k_{eff}	k_{eff}	Tf (K)	k_{eff}	k_{eff}
560	1.0002	1.0002	560	1.0328	1.0356
565	1.0000	1.0000	565	1.0326	1.0354
570	0.9999	0.9999	570	1.0324	1.0352
575	0.9997	0.9997	575	1.0323	1.0350
580	0.9996	0.9996	580	1.0321	1.0349
585	0.9994	0.9994	585	1.0319	1.0347
590	0.9993	0.9993	590	1.0317	1.0345
Boron (ppm)	2010.6	2202.1	Boron (ppm)	30.2	5.3
DTC (pcm/K)	-2.96	-2.98	DTC (pcm/K)	-3.27	-3.34

4.5.2 Moderator Temperature and Density Reactivity Coefficients

Figure 22 and Figure 23 depict the reactivity results, calculated using Eq. 1, as functions of moderator temperature for both the LEU and LEU+ cores at ZPPT and EOC conditions, respectively. Figure 24 and Figure 25 show the same reactivity results but as functions of moderator density for both the LEU and LEU+ cores at ZPPT and EOC conditions, respectively. Table 8 summarizes the k_{eff} results for the cases shown in these two figures, and also the critical boron concentrations and MTCs. Zero core power and constant fuel temperature (565 K) were used in these ZPPT and EOC cases. The same critical boron concentrations and Xe and Sm concentrations described in the previous subsection were used in the respective ZPPT and EOC cases here. As shown in Table 8, the moderator temperature and density were correlated (shown in the first two columns) [11] and thus changed simultaneously from one case to another. k_{eff} decreased in all four cases as moderator temperature increased from 550 to 580 K, which is expected because higher temperature leads to decreased moderator density, which reduces the neutron moderation. As expected, k_{eff} increased when moderator density increased. The MTCs were derived by calculating the value of the first derivative of fitting functions (shown in Figure 22 and Figure 24) at a given temperature. Given that the fitting functions are second-order polynomials, the MTCs are different at different moderator temperatures. As shown in Table 8, the MTCs of both cores are much higher (i.e., more negative) at EOC than at ZPPT, and they were significantly higher in the LEU+ core than in the LEU core at both ZPPT and EOC conditions. Similar to this study, Phase 1 study [4] also shows higher magnitudes in MTC at higher burnups. However, the trend of MTC with enrichment is different between this study and Phase 1 study because Phase 1 study shows lower MTC magnitudes in higher enrichment cases. Such difference can be attributed to the simplifications used in Phase 1 study described in Subsection 4.5.1.

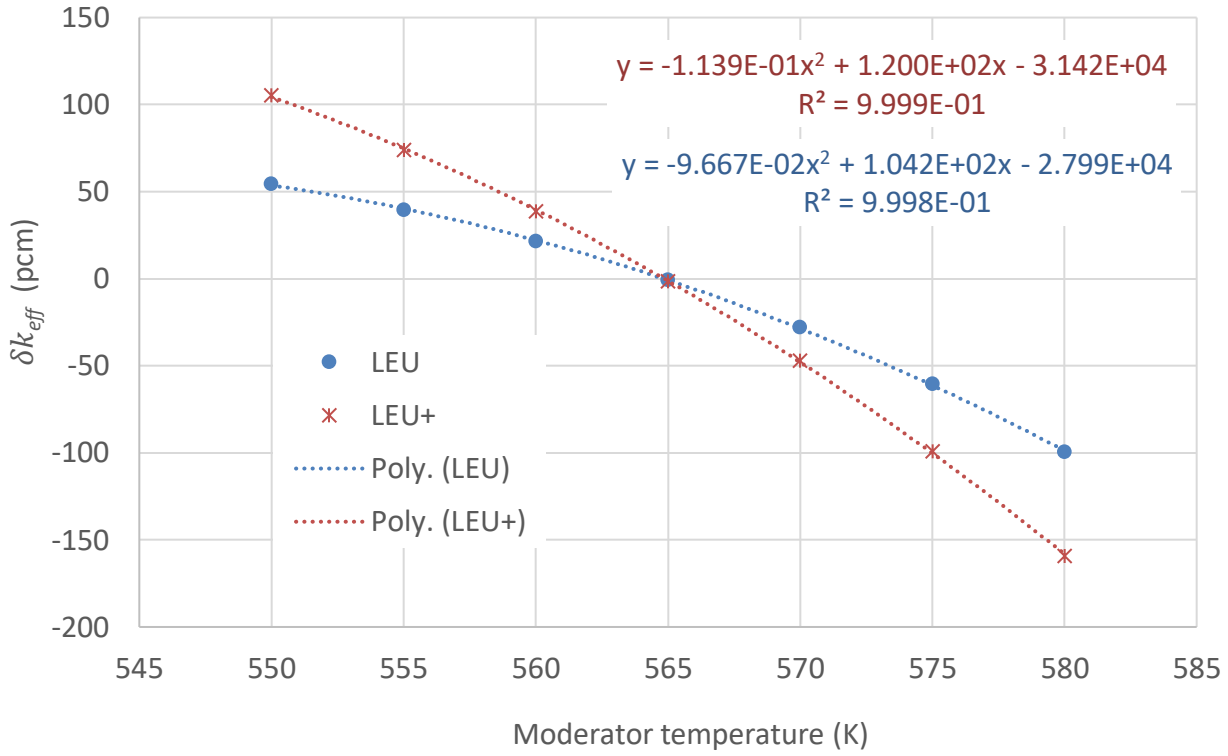

Figure 22. Reactivity as a function of moderator temperature calculated by PARCS for the LEU and LEU+ cores at ZPPT. The fitting equation in red is for the LEU+ core.

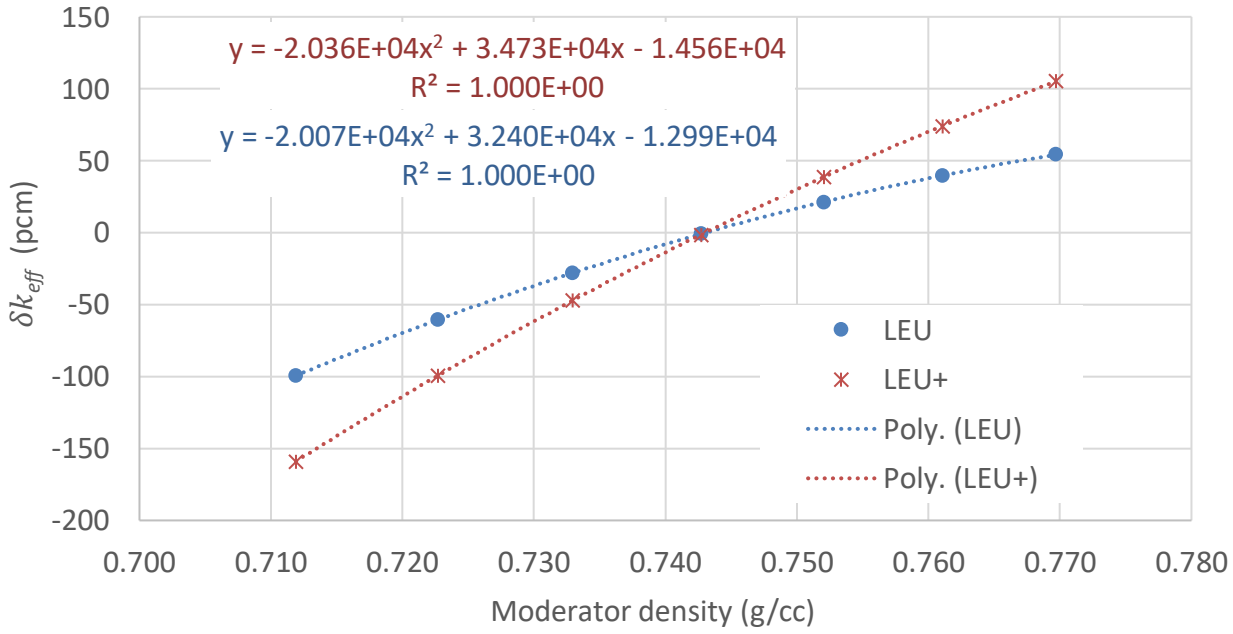

Figure 23. Reactivity as a function of moderator density calculated by PARCS for the LEU and LEU+ cores at ZPPT. The fitting equation in red is for the LEU+ core.

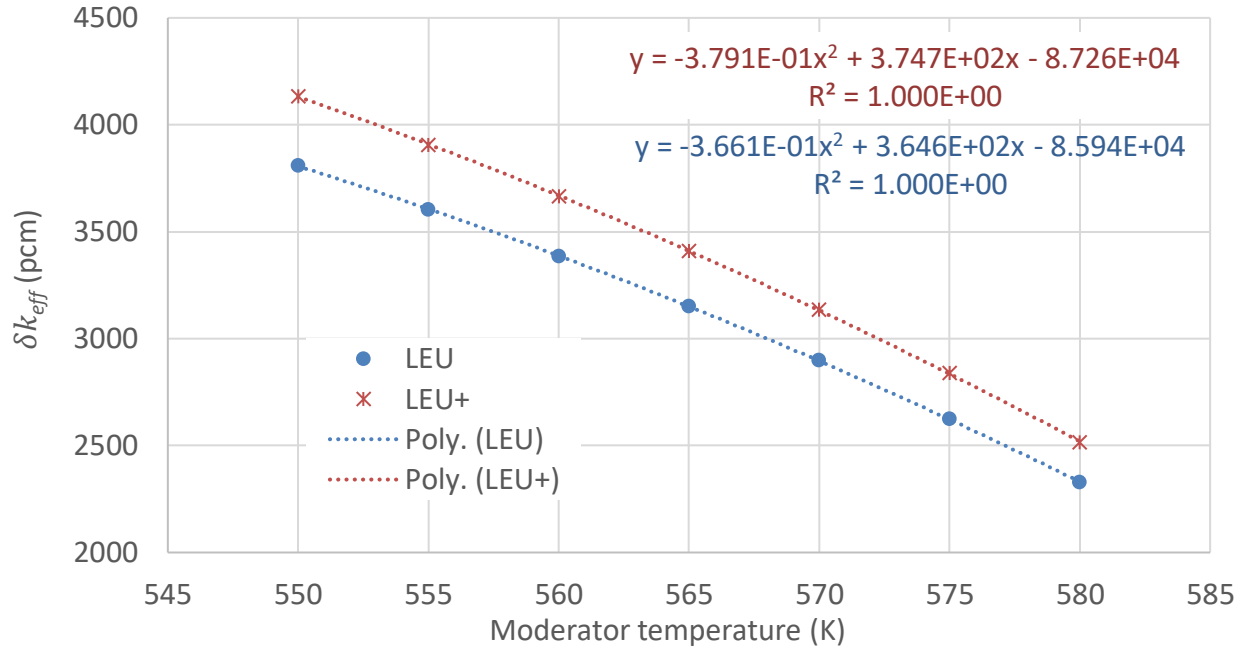

Figure 24. Reactivity as a function of moderator temperature calculated by PARCS for the LEU and LEU+ cores at EOC. The fitting equation in red is for the LEU+ core.

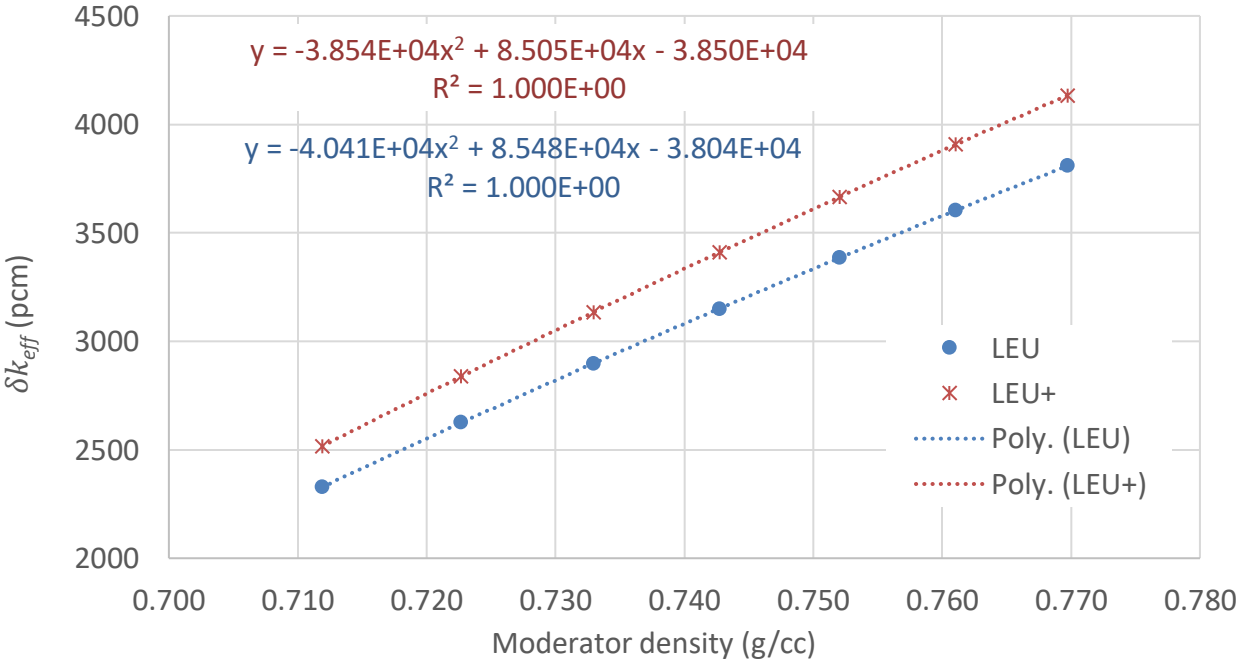

Figure 25. Reactivity as a function of moderator density calculated by PARCS for the LEU and LEU+ cores at EOC. The fitting equation in red is for the LEU+ core.

Table 8. k_{eff} as a function of moderator temperature and density calculated by PARCS for the LEU and LEU+ cores at the ZPPT and EOC conditions. The critical boron concentrations and MTCs at 565 K are also shown.

ZPPT				EOC			
		LEU	LEU+			LEU	LEU+
Tm (K)	Density (g/cc)	k_{eff}	k_{eff}	Tm (K)	Density (g/cc)	k_{eff}	k_{eff}
550	0.7697	1.0005	1.0011	550	0.7697	1.0396	1.0431
555	0.7611	1.0004	1.0007	555	0.7611	1.0374	1.0407
560	0.7521	1.0002	1.0004	560	0.7521	1.0350	1.0381
565	0.7427	1.0000	1.0000	565	0.7427	1.0325	1.0353
570	0.7329	0.9997	0.9995	570	0.7329	1.0299	1.0324
575	0.7227	0.9994	0.9990	575	0.7227	1.0270	1.0292
580	0.7119	0.9990	0.9984	580	0.7119	1.0238	1.0258
Boron concentration (ppm)		2010.6	2202.1	Boron concentration (ppm)		30.2	5.3
MTC at 565K (pcm/K)		-5.04	-8.71	MTC at 565K (pcm/K)		-49.09	-53.68

4.5.3 Control Rod Worth

Figure 26 shows the CRW results for each of the nine control banks for the LEU and LEU+ cores at both BOC and EOC. Table 9 summarizes the CRW results, the critical boron concentrations of each case, and k_{eff} of the reference cases, which had all control rods out/withdrawn (ARO). Critical boron concentrations and the Xe/Sm concentrations from the corresponding HFP cases were read from history files into these CRW cases that were simulated at HZP conditions. To calculate CRW, one of the nine control banks was fully inserted in the core in each case. Each control bank can appear in one or more assemblies, as shown in Figure 7. For instance, control bank A appears in two assemblies at F-8 and H-10 locations in the southeast quadrant. In this study, control bank A at both assemblies was treated as a whole and inserted at once to calculate k_{eff}, which was then compared with the k_{eff} of the reference case (i.e., the corresponding ARO case, k_{eff_ref}). Similar treatments were performed on other control banks. The CRW (in pcm) is calculated using Eq.2 below.

$$CRW = (1/k_{eff} - 1/k_{eff\_ref}) \times 10^5 \quad \text{(Eq. 2)}$$

Each control bank has a different CRW because of the different locations and the different number of hosting assemblies that each control bank has. At BOC, the CRW is similar between LEU and LEU+ for most corresponding banks, except for banks B, C, and D, which had >16% differences. At EOC, CRWs of LEU+ are 19 to 50% lower than those of LEU for all banks, except for bank SA. This is likely caused by higher amounts of the neutron-absorbing fission products accumulated in LEU+ with higher EOC burnups than LEU, which lead to higher competition of neutron absorptions with the control banks in LEU+. Control banks C and SB had the largest CRWs for both LEU and LEU+ at BOC and EOC. Similar to this study, Phase 1 study [4] also shows higher magnitudes in CRW at higher burnups. However, the trend of CRW with enrichment is different between this study and Phase 1 study because Phase 1 study shows lower CRW magnitudes in higher enrichment cases. Such difference can be attributed to the simplifications used in Phase 1 study described in Subsection 4.5.1.

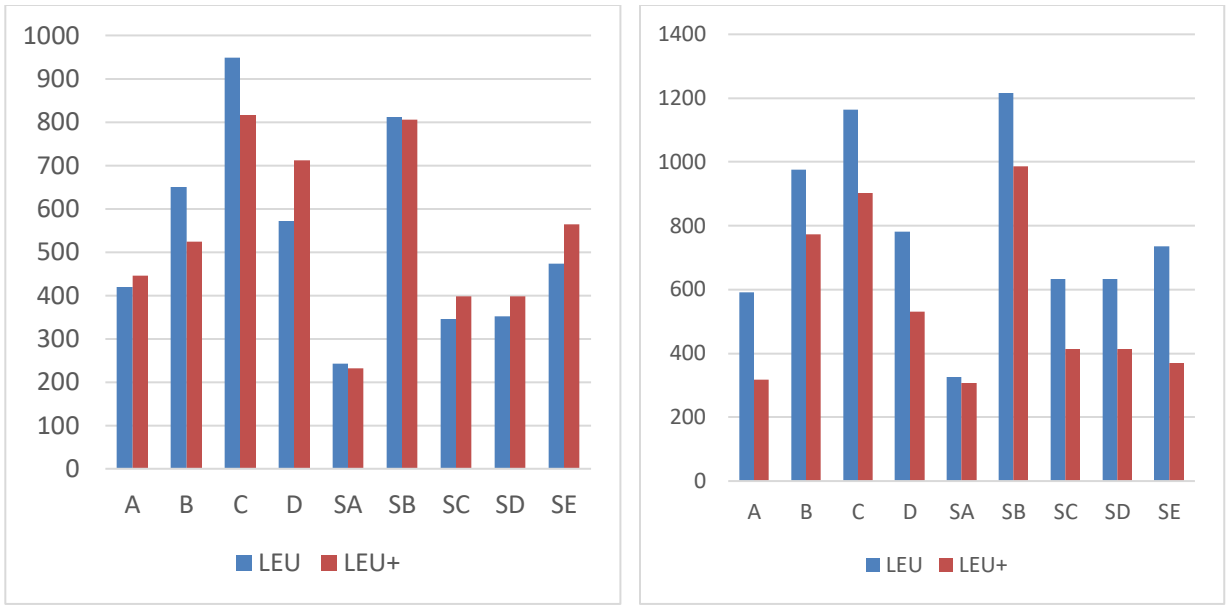

(a) BOC (b) EOC

Figure 26. The CRW (pcm) for each control bank for both LEU and LEU+ cores calculated by PARCS at (a) BOC and (b) EOC.

Table 9. k_{eff} when each control bank is inserted and the CRW (pcm) for each control bank for both LEU and LEU+ cores calculated by PARCS at BOC and EOC. k_{eff} for the reference cases (HZP_ARO) and the critical boron concentrations are also included.

BOC						EOC					
	LEU		LEU+		CRW		LEU		LEU+		CRW
Bank name	k_{eff}	CRW (pcm)	k_{eff}	CRW (pcm)	(LEU+/ LEU-1)%	Bank name	k_{eff}	CRW (pcm)	k_{eff}	CRW (pcm)	(LEU+/ LEU-1)%
A	1.0113	420.2	1.0138	445.6	6.0	A	1.0263	592.2	1.0319	318.0	-46.3
B	1.0089	649.6	1.0130	523.9	-19.4	B	1.0223	975.9	1.0271	773.9	-20.7
C	1.0059	948.3	1.0100	815.9	-14.0	C	1.0204	1163.5	1.0257	903.3	-22.4
D	1.0097	572.3	1.0111	712.5	24.5	D	1.0243	781.6	1.0297	531.1	-32.0
SA	1.0131	243.2	1.0160	232.2	-4.5	SA	1.0292	325.3	1.0320	307.3	-5.5
SB	1.0073	811.1	1.0101	805.2	-0.7	SB	1.0198	1215.3	1.0249	985.9	-18.9
SC	1.0120	345.4	1.0143	398.2	15.3	SC	1.0259	634.1	1.0309	413.7	-34.8
SD	1.0120	351.6	1.0143	398.5	13.3	SD	1.0259	634.0	1.0309	413.7	-34.7
SE	1.0107	473.2	1.0126	564.4	19.3	SE	1.0248	734.9	1.0314	369.1	-49.8
Sum		4814.9		4896.3	1.7	Sum		7056.7		5016	-28.9
		LEU		LEU+				LEU		LEU+	
k_{eff_ref} (HZP_ARO)		1.01558		1.018386		$k_{eff\ \_ref}$ (HZP_ARO)		1.03261		1.03532	
Boron (ppm)		1241.4		1237		Boron (ppm)		30.2		5.2	

4.5.4 Shutdown Margin

A four-step procedure, which was simplified from Section 4.3 of the NRC's standard review plan [14], was followed in this work to calculate the SDM. These four steps are the following:

- Step 1 (S1): HFP with ARO condition (HFP_ARO) was used to calculate the critical boron concentration and the equilibrium Xe/Sm concentrations at both BOC and EOC, which were then fed through a history file into the next three steps. k_{eff} is also calculated for this case.

- Step 2 (S2): using the boron and Xe/Sm concentrations from Step 1, k_{eff} was calculated in this step under the HZP and ARO (HZP_ARO) conditions.

- Step 3 (S3): using the boron and Xe/Sm concentrations from Step 1, k_{eff} was calculated in this step under the HZP conditions with all control rods were inserted (ARI).

- Step 4 (S4): using the boron and Xe/Sm concentrations from Step 1, k_{eff} was calculated in this step under the HZP conditions with all control rods, except for the bank with the highest worth, inserted (worst rod stuck out, or WRSO).

For simplicity, bank SB was used as the bank with the highest worth for all cases for consistency in this calculation, even though bank C had slightly higher worth than bank SB at BOC, as shown in the previous section. Using Eq. 2, the relative difference in k_{eff} between S2 and S1 was calculated, which was caused by the differences in fuel temperature and moderator temperature and density between these two

steps. The difference in k_{eff} is often referred to as moderator and fuel temperature defect. The relative difference in k_{eff} between S3 and S2 was caused by insertion of all the control rods, which can be considered as the integral CRW. Relative difference in k_{eff} between S4 and S2 was caused by insertion of all the control rods, except bank SB, which can be considered as the SDM.

Table 10 shows the k_{eff} results for the cases corresponding to each of these four steps for both the LEU and LEU+ cores at BOC and EOC. The relative differences in k_{eff}, including SDM, between the corresponding cases are also included. This table also includes the critical boron concentration, core average moderator temperature and density, and core average fuel temperature used in these cases. Significantly higher SDMs are seen at EOC than BOC.

Table 10. k_{eff} of the four cases used to calculate SDM for both LEU and LEU+ cores at both BOC and EOC. The moderator and fuel temperature defect, integral CRW, and SDM for the LEU and the LEU+ cores were calculated by PARCS at both BOC and EOC. The boron concentration and fuel and moderator conditions used in these cases are also included.

		BOC		EOC	
Step ID	Step name	k_{eff} (LEU)	k_{eff} (LEU+)	k_{eff} (LEU)	k_{eff} (LEU+)
S1	HFP_ARO	1.0000	1.0000	1.0000	1.0000
S2	HZP_ARO	1.0156	1.0184	1.0326	1.0353
S3	HZP_ARI	0.9529	0.9564	0.9553	0.9623
S4	HZP_WRSO	0.9611	0.9661	0.9676	0.975397526
		pcm (LEU)	pcm (LEU+)	pcm (LEU)	pcm (LEU+)
S2 vs. S1	Mod. and fuel defect	1534	1805	3158	3412
S3 vs. S2	Integral CRW	6473	6362	7834	7331
S4 vs. S2	**SDM**	**5583**	**5317**	**6503**	**5948**
		LEU (BOC)	LEU+ (BOC)	LEU (EOC)	LEU+ (EOC)
	Critical boron (ppm)	1,241	1,273	30	5
HFP	Fuel temp. (K)	858	860	856	856
	Mod. temp. (K)	584	585	585	585
	Mod. density (g/cc)	0.6996	0.6985	0.6992	0.6992
HZP	Fuel temp. (K)	565	565	565	565
	Mod. temp. (K)	565	565	565	565
	Mod. density (g/cc)	0.7430	0.7430	0.7430	0.7430

5. SUMMARY AND CONCLUSIONS

A representative high-burnup PWR core design with LEU+ fuel (with 5.95–6.6% enrichments) and a 24-month fuel cycle developed by SNC was modeled and simulated in this work using the Polaris, GenPMAXS, and PARCS code suite. A representative LEU (with 4.2–4.6 enrichments) PWR core design with an 18-month fuel cycle was also modeled to serve as a reference for the LEU+ case. Nine different fuel assembly designs with different combinations of enrichments, numbers of IFBA rods, and numbers of WABA rods were used in the LEU+ and the LEU cores. As expected, a higher number of IFBA rods and WABA rods were used in the LEU+ core than in the LEU core. Polaris was used to model these assembly types at various reactor operating conditions and branches to generate the cross section files, which were then processed by GenPMAXS to generate the nodal cross section data required for the PARCS simulations. The PARCS results show that the average specific powers in all three fuel batches in the LEU+ core were similar to the corresponding fuel batches in the LEU core when the total core powers and total uranium loadings in both cores were the same. Representative three-batch fuel shuffling schemes were simulated by PARCS, and reactor core simulations were performed using PARCS to reach an equilibrium cycle for both LEU+ and LEU cores and then deplete them. The PARCS results for both cores at ZPPT, BOC, and EOC conditions were presented in this report, including results for boron concentrations, burnup distributions, power peaking factors, reactivity coefficients, CRW, and SDM.

The PARCS results for the LEU+ core were first compared with VERA results for the same core for verification purposes. Generally good agreements between the VERA and PARCS results were seen in the soluble boron and radial burnup distribution. The PARCS results were also compared between the LEU+ and LEU cores, and the following conclusions were made based on the core designs studied in this work. A more comprehensive comparisons of the core physics characteristics between the two cores are summarized in Table 11.

- The cycle length of the LEU+ core was estimated to be 704 EFPD with a core average burnup accumulation of 28.43 GWd/MTU. The cycle length of the LEU core was estimated to be 514 EFPD with an average burnup accumulation of 20.70 GWd/MTU.
- The critical boron concentrations were found to be much higher in the LEU+ core than in the LEU core after ~100 EFPDs in a cycle (e.g., 1582 vs. 1335 ppm for peak values).
- Much higher EOC burnups were found in the LEU+ core than in the LEU core (71.45 vs. 51.63 GWd/MTU for peak values).
- Higher assembly radial power peaking factors (1.40 vs. 1.30 for peak values), 2D pin peaking factors (1.53 vs. 1.42 for peak values), and 3D pin peaking factors (1.89 vs. 1.81 for peak values) were found in the LEU+ core than in the LEU core.
- Similar DTCs were found between LEU+ and LEU (e.g., -2.96 vs. -2.98 pcm/K at ZPPT). Significantly higher MTCs were found in LEU+ than in LEU (e.g., -8.71 vs. -5.04 pcm/K at ZPPT).
- Similar CRWs were found between LEU+ and LEU at BOC for most control banks, except banks B, C, and D. Significantly lower CRWs at EOC were found in LEU+ than in LEU for all but one control bank (e.g., 531 vs. 782 pcm for bank D).
- Lower SDMs were found in the LEU+ core than in LEU core (e.g., 5948 vs. 6503 pcm at EOC).

This report also provides a demonstration of the current state of the Polaris/GenPMAXS/PARCS code suite in modeling PWR cores under steady-state operations. This work also contributed to Polaris/GenPMAX/PARCS improvements by providing feedback on code performances and also feature requests for a core physics study based realistic core designs.

A key lesson learned in this work is how to approach equilibrium cycle using PARCS. This work used two trial cycles to “jump start” the iteration for equilibrium cycle search (described in Section 4). It was

later discovered that such trial cycles are not needed and the following precedure can be used to approach equilibrium cycle using PARCS: start with a fresh core filled the same assembly type, deplete for a cycle, shuffle in fresh assemblies of the desired types, and iterate the core depletion cycle and fuel shuffle until the burnup distributions converge between two subsequent cycles. The converged core can be treated as an equilibrium cycle of the given core layouts and shuffle scheme.

Table 11. Summary of the LEU and LEU+ core physics characteristics.

Parameter	LEU core	LEU+ core
Plant Rating (MWth)	3626	3626
Cycle Length (months)	18	24
Cycle Length (EFPD)	514	704
Number of Assemblies in Core	193	193
Fresh Fuel Enrichment (wt%)	4.2/4.6	5.95/6.2/6.6
Core average enrichment (wt%)	4.4	6.0
Total U loading/assembly (MT)	0.465	0.465
Number of Fuel Batches	3	3
Fresh|Once-burned|Twice-burned batch at BOC	89|92|12	85|84|24
Average Assembly Discharge Burnup (GWd/MTU)	45.2	63.2
Max Assembly Discharge Burnup (GWd/MTU)	50.1	71.5
Core average burnup at EOC (GWd/MTU)	35.8	50.5
Average Specific Power (MW/MTU)	40.3	40.4
Cycle Burnup Accumulation (GWd/MTU) (Fresh|Once-burned|Twice-burned fuel batch)	24.8|18.4|8.1	34.3|27.6|10.4
Cycle-average Specific Power (MW/MTU) (Fresh|Once-burned|Twice-burned fuel batch)	48.3|35.8|15.8	48.8|39.2|14.8
Max critical boron concentration (ppm)	1335	1582
Max assembly radial peaking factor	1.30	1.40
Max 2D pin peaking factor	1.42	1.53
Max 3D pin peaking factor	1.81	1.89
DTC (pcm/K) at ZPPT|EOC	-2.96|-3.27	-2.98|-3.34
MTC (pcm/K) at 565K at ZPPT|EOC	-5.04|-49.09	-8.71|-53.68
Integral CRW (pcm) at BOC|EOC	6473|7834	6362|7331
SDM (pcm) at BOC|EOC	5583|6503	5317|5948

ACKNOWLEDGMENTS

Support for this work was provided by the NRC's Offices of Nuclear Regulatory Research, Nuclear Reactor Regulation, and Nuclear Material Safety and Safeguards. The LEU+ core modeled in this work was developed by Southern Nuclear Company (SNC). The authors would also like to thank Andrew Godfrey of ORNL for his help with core designs and review, Andrew Ward of University of Michigan for his help with PARCS usage, Andrew Bielen of NRC for his feedback on PARCS modeling, Nicholas Szewczyk of SNC for his technical review and feedback on the results, Germina Ilas of ORNL for her thorough review, and Erik Walker and Mehdi Asgari of ORNL for their valuable feedback to this work.

REFERENCES

[1] U. Mertyurek, M. Jessee and B. Betzler, "Lattice physics calculations using the embedded self-shielding method in Polaris, Part II: Benchmark assessment," *Annals of Nuclear Energy, https://doi.org/10.1016/j.anucene.2020.107829,* vol. 150, no. 107829, 2021.

[2] M. Jessee, W. Wieselquist, U. Mertyurek, K. S. Kim, T. Evans, S. Hamilton and C. Gentry, "Lattice physics calculations using the embedded self-shielding method in Polaris, Part I: Methods and implementation," *Annals of Nuclear Energy, https://doi.org/10.1016/j.anucene.2020.107830,* vol. 150, no. 107830, 2021.

[3] T. Downar, et al., "PARCS, NRC - v3.3.2 Release," University of Michigan, Ann Arbor, MI, 2020.

[4] R. Hall, R. Cumberland, R. Sweet and W. Wieselquist, "Isotopic and Fuel Lattice Parameter Trends in Extended Enrichment and Higher Burnup LWR Fuel, Vol. 1: PWR Fuel," Oak Ridge National Laboratory, ORNL/TM-2020/1833, Oak Ridge, TN, 2021.

[5] R. Cumberland, R. Sweet, U. Mertyurek, R. Hall and W. Wieselquist, "Isotopic and Fuel Lattice Parameter Trends in Extended Enrichment and Higher Burnup LWR Fuel, Vol. II: BWR Fuel," Oak Ridge National Laboratory, ORNL/TM-2020/1835, Oak Ridge, TN, 2021.

[6] N. Capps, et al., "Full core LOCA safety analysis for a PWR containing high burnup fuel," *Nuclear Engineering and Design,* vol. 379, no. 111194. https://doi.org/10.1016/j.nucengdes.2021.111194, 2021.

[7] Y. Xu and T. Downar, "GenPMAXS-V6, Code for Generating the PARCS Cross Section Interface File PMAXS," University of Michigan, Ann Arbor, MI, 2012.

[8] W. Wieselquist, R. Lefebvre and M. Jessee, "SCALE Code System, version 6.2.4," Oak Ridge National Laboratory, ORNL/TM-2005/39, Oak Ridge, TN, April 2020.

[9] U.S. Nuclear Regulatory Commission, "TRACE V5.840 User's Manual, Volume 1: Input Specification," Washington DC, 2014.

[10] U.S. Nuclear Regulatory Commission, "RELAP5/MOD3.3 Code Manual, Volumes I through VIII," Washington DC, 2016.

[11] A. Godfrey, "VERA Core Physics Benchmark Progression Problem Specifications," Oak Ridge National Laboratory, CASL-U-2012-0131-004, Oak Ridge, TN, 2014.

[12] C. Sanders and J. Wagner, "Study of the Effect of Integral Burnable Absorbers for PWR Burnup Credit," U.S. Nuclear Regulatory Commission, NUREG/CR-6760, https://www.nrc.gov/reading-rm/doc-collections/nuregs/contract/cr6760/index.html#pub-info, Washington DC, 2001.

[13] J. Skutch, W. Slagle and Y. Sung, "TVA Watts Bar Unit 1 Cycle 2 Reload Safety Evaluation," Westinghouse Electric Corporation, https://www.nrc.gov/docs/ML0734/ML073460287.pdf, Pittsburgh, PA, 1997.

[14] U.S. NRC, "U.S. NRC Standard Review Plan, Section 4.3 Nuclear Design," NRC, NUREG-0800, https://www.nrc.gov/docs/ML0707/ML070740003.pdf, Washington DC, 2007.

APPENDIX A. RESULTS FOR THE EVEN CYCLE FOR THE LEU+ CORE

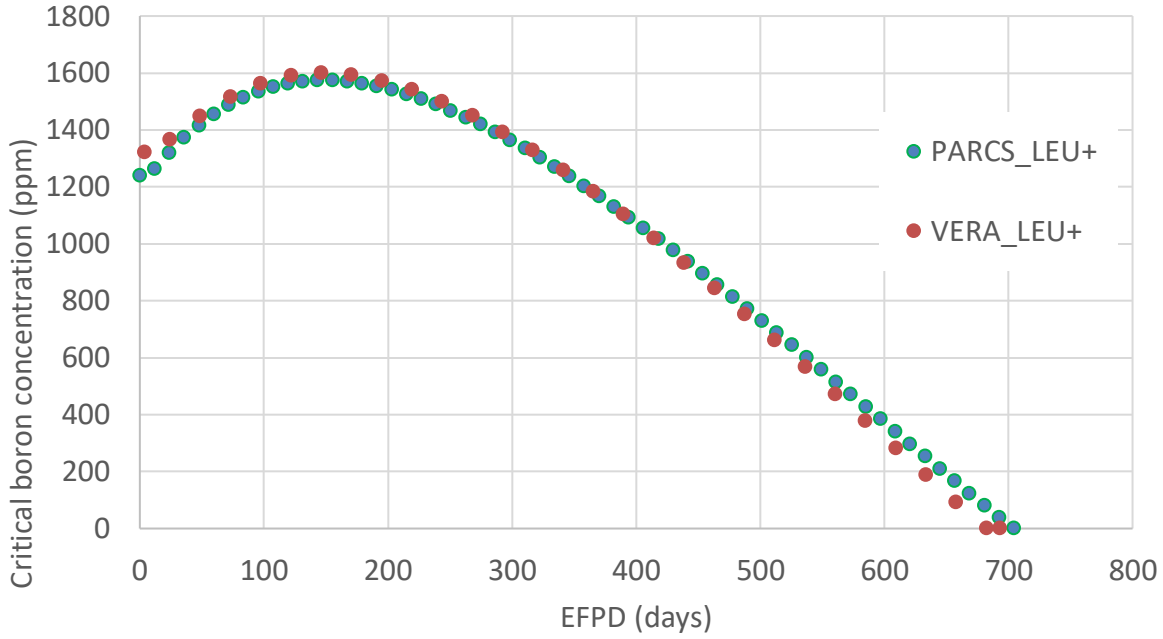

Figure A.1. Critical soluble boron concentrations of the LEU+ core (even cycle) calculated by PARCS and VERA.

	H	G	F	E	D	C	B	A
8	37.41	34.33	0.00	34.77	33.44	37.42	0.00	37.96
9	34.23	0.00	34.86	0.00	29.02	0.00	0.00	37.96
10	0.00	34.86	0.00	35.22	0.00	33.49	0.00	55.48
11	34.79	0.00	34.77	34.23	32.03	0.00	0.00	63.12
12	33.45	29.12	0.00	32.05	28.86	0.00	37.56	
13	37.59	0.00	33.55	0.00	0.00	0.00	53.03	
14	0.00	0.00	0.00	0.00	37.60	53.02		
15	37.96	37.13	55.51	63.13				

(a) PARCS

H	G	F	E	D	C	B	A
38.20	34.55	0.00	36.28	34.30	38.36	0.00	38.38
34.79	0.00	35.05	0.00	29.49	0.00	0.00	38.74
0.00	35.06	0.00	35.68	0.00	34.18	0.00	55.65
34.30	0.00	35.30	34.66	32.71	0.00	0.00	63.60
34.31	29.60	0.00	32.75	29.49	0.00	38.10	
38.19	0.00	34.10	0.00	0.00	0.00	53.49	
0.00	0.00	0.00	0.00	38.13	53.49		
39.11	37.67	55.70	63.60				

(b) VERA

Figure A.2. The average burnup in each assembly at BOC in the LEU+ core (even cycle) calculated by (a) PARCS and (b) VERA.

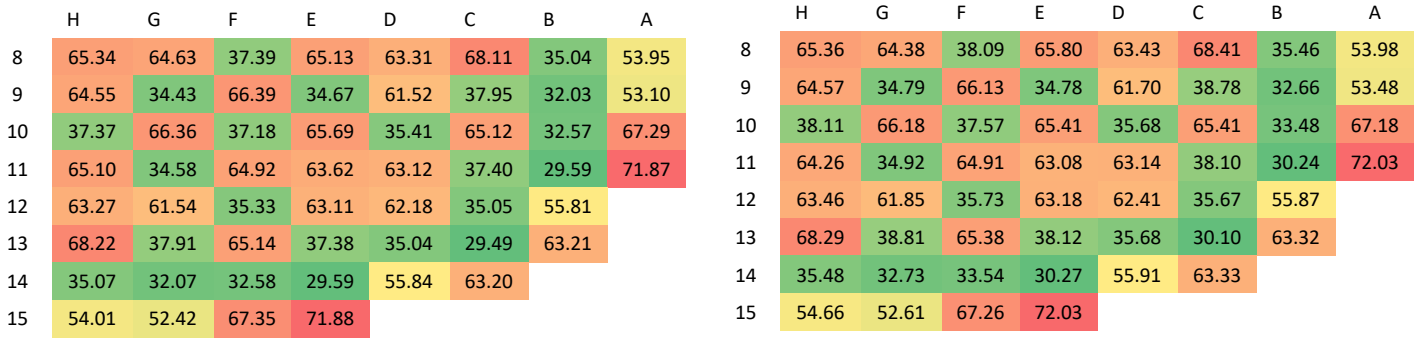

(a) PARCS (b) VERA

Figure A.3. The average burnup in each assembly at EOC in the LEU+ core (even cycle) calculated by (a) PARCS and (b) VERA.

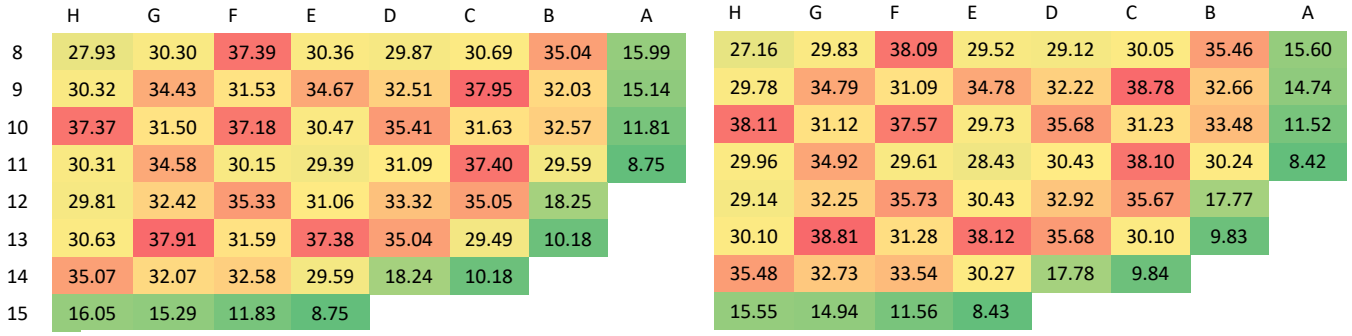

(a) PARCS (b) VERA

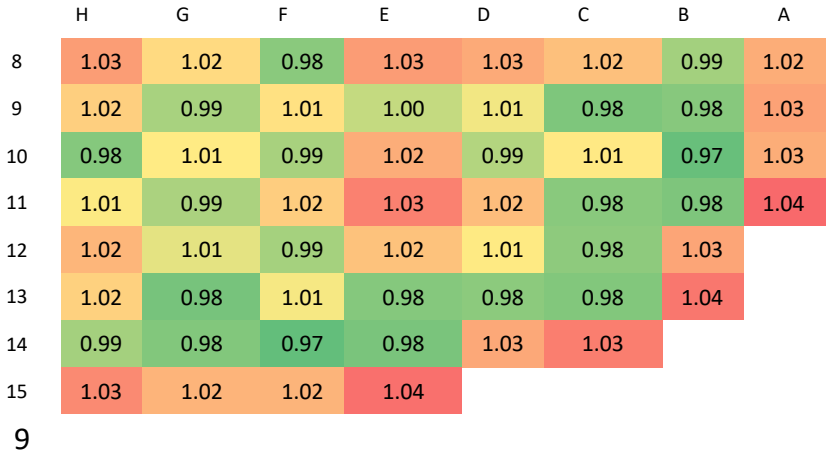

(c) burnup ratio of PARCS to VERA

Figure A.4. The burnup accumulated in an equilibrium cycle in each assembly in the LEU+ core (even cycle) calculated by (a) PARCS and (b) VERA; (c) the ratio of burnup accumulation calculated by PARCS to that by VERA.

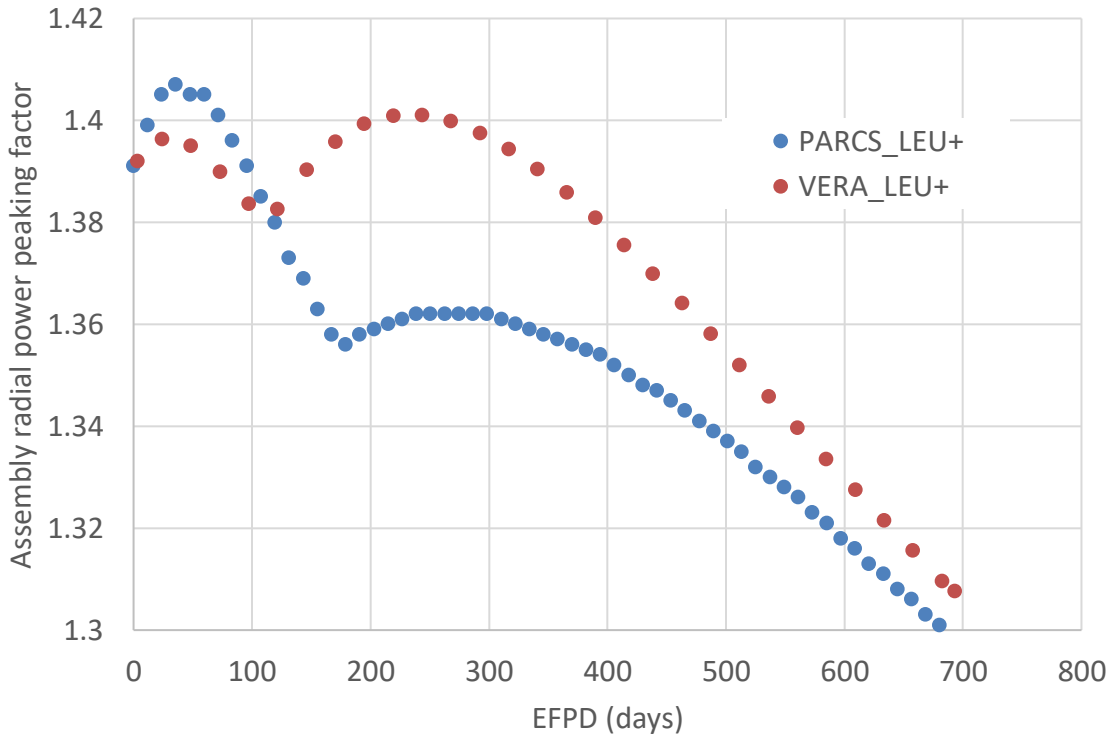

Figure A.5. Assembly radial power peaking factor integrated over the assembly height as a function of EFPD for the LEU+ core (even cycle) calculated by PARCS and VERA.

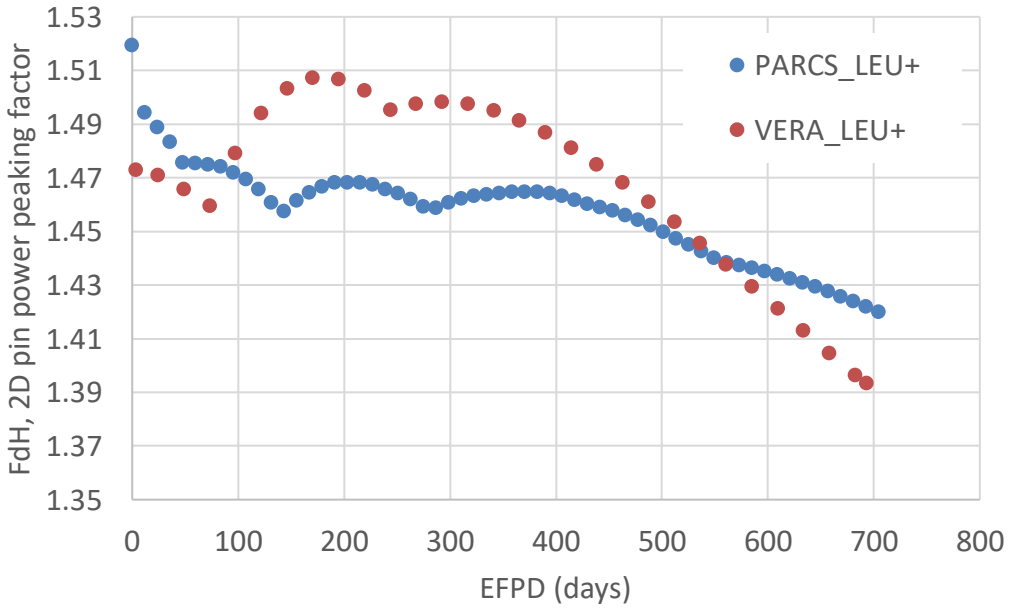

Figure A.6. 2D pin power peaking factor (FdH) integrated over the pin height as a function of EFPD for the LEU+ core (even cycle) calculated by PARCS and VERA.

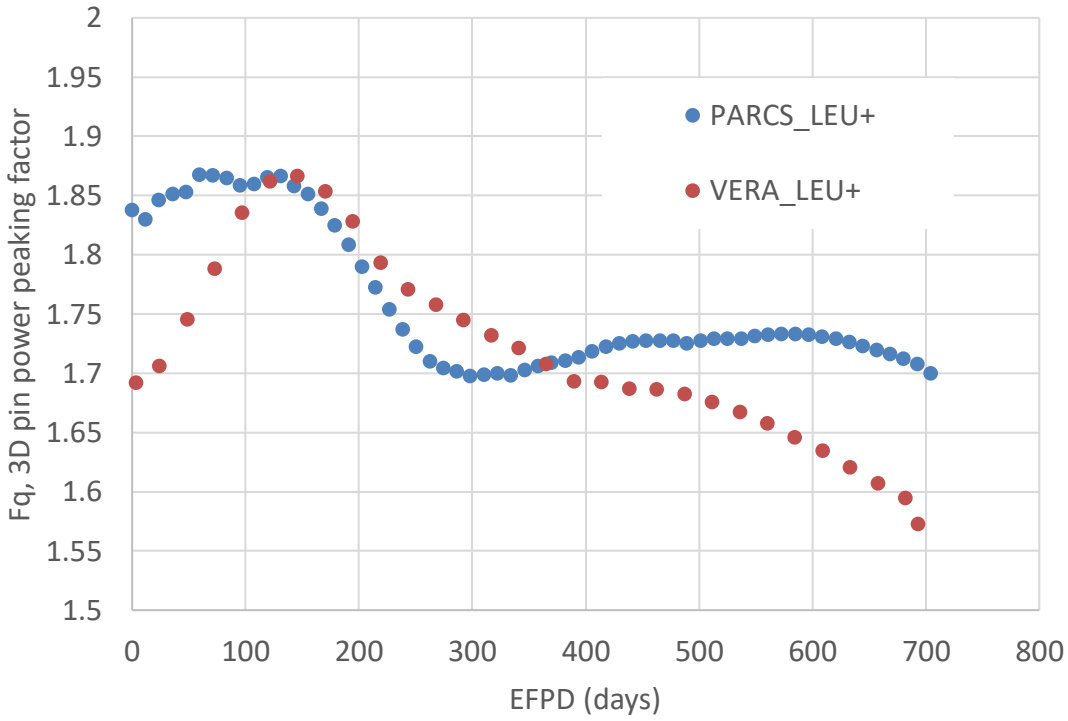

Figure A.7. 3D pin power peaking factor (Fq) among axial pin segments as a function of EFPD for the LEU+ core (even cycle) calculated by PARCS and VERA.

APPENDIX B. DESCRIPTION OF THE REPOSITORY

All input and output files that relevant to this work is stored in a Gitlab repository. The overall file structure is shown in Fig. B.1. As shown, the overall directory "HALEU_PWR_fullCore" for this work contains an Excel file that includes all the results presented in this report, and it also contains two subdirectories: "LEU_files" stores the files for the LEU core studied in this work and "LEU+_files" stores the files for the LEU+ core. "LEU_files" and "LEU+_files" have the same three subdirectories: "GenPMAX", "Parcs", and "Polaris". As indicated by the directory names, "GenPMAX" stores the input/output files of the GenPMAXS calculations to generate the PMAXS files used by PARCS calculations (Fig. B.2); "Parcs" stores the input/output files of the PARCS core calculations (Fig. B.1); "Polaris" stores the input/output files of the Polaris calculations to generate the T16 files from each fuel assembly types and their associated branch cases (Fig. B.3). There are "readme" files in most subdirectories that explain what the files are.

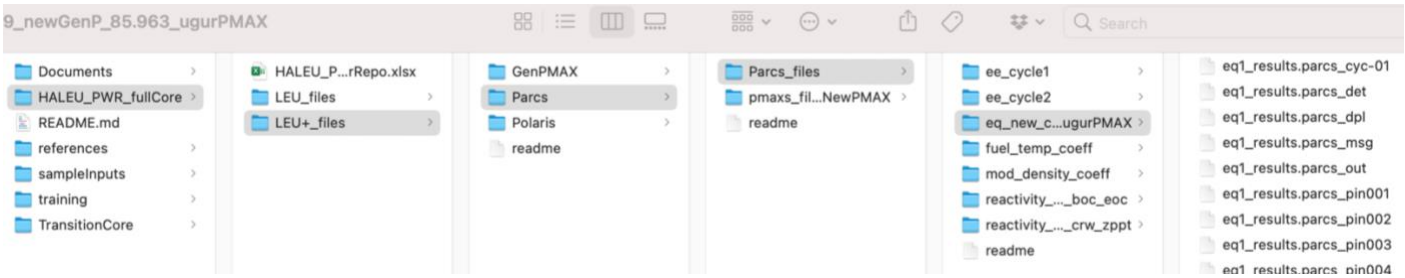

Figure B.1. Overall directory of the files related to this work stored in a Gitlab repository. Note that the files in the right-most column were truncated for brevity.

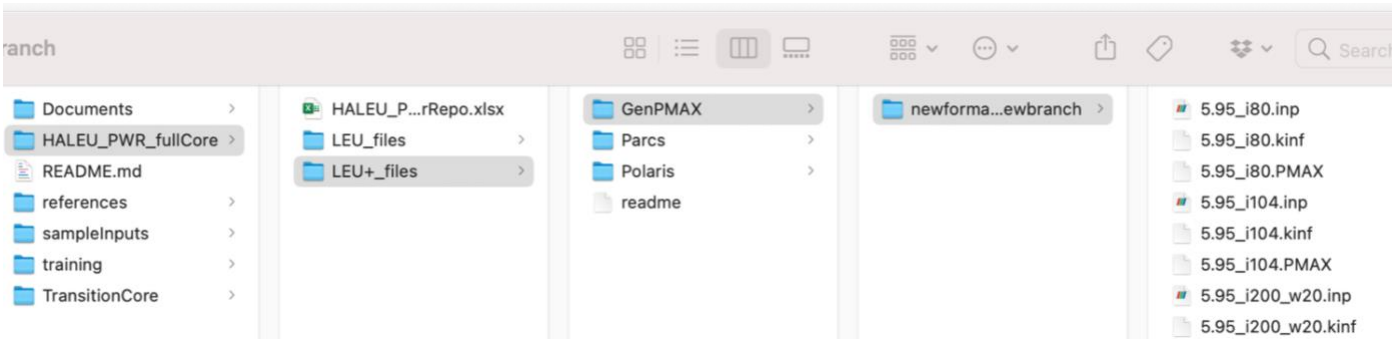

Figure B.2. Details of subdirectory "GenPMAX" of the Gitlab repository. Note that the files in the right-most column were truncated for brevity.

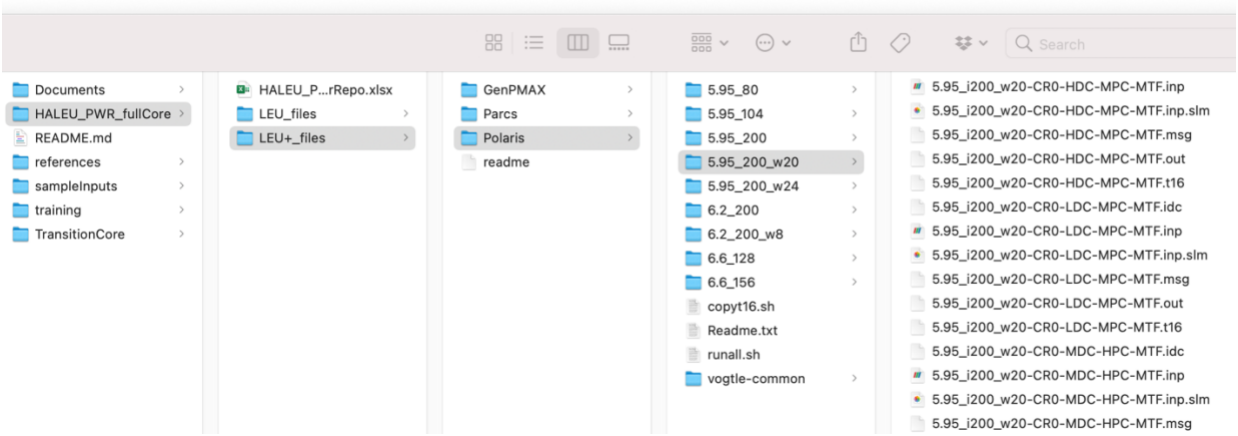

Figure B.3. Details of subdirectory "Polaris" of the Gitlab repository. Note that the files in the right-most column were truncated for brevity.